Contributions of gluon recombination to saturation phenomena

Wei Zhu, **Jianhong Ruan**, **Jifeng Yang** and **Zhenqi Shen**

Department of Physics, East China Normal University, Shanghai 200062, P.R. China

Abstract

Parton distributions in the small x region are numerically predicted by using a modified DGLAP equation with the GRV-like input distributions. We find that gluon recombination at twist-4 level obviously suppresses the rapid growth of parton densities with x decrease. We show that before the saturation scale Q_s^2 is reached, saturation and partial saturation appear in the small x behavior of parton distributions in nucleus and free proton, respectively. The antishadowing contributions to the saturation phenomena are also discussed.

PACS numbers: 12.38.Bx, 24.85.+p

1 Introduction

The QCD evolution equations for parton densities at twist-2 level, both the DGLAP equation [1] and BFKL equation [2] predict a rapid increase of the parton densities in the small x region due to parton splitting, and the unitarity limit is violated. Therefore, the corrections of the higher order QCD effects, which suppress or shadow the growth of parton densities, become a focus of intensive study in recent years. An important character at the small x limit is that the suppressed parton distributions approach a limiting form and unitarity is restored. This is called saturation.

There are various ways to define and analyze the saturation phenomena based on perturbative QCD [3,4]. The shadowing corrections of gluon recombination to the integrated parton distributions were mainly studied by adding nonlinear terms in the DGLAP evolution equation in the collinear factorization scheme. A pioneering work in this aspect was derived by Gribov, Levin and Ryskin in [5] and by Mueller and Qiu [6] at the twist-4 level. The GLR-MQ equation sums the contributions of gluon recombination diagrams using the AGK (Abramovsky, Gribov, Kancheli) cutting rule [7]. In the next step, the contributions of multi-parton correlations are summed by using the Glauber model in Mueller's works [8] and this Glauber-Mueller equation reduces to the GLR-MQ equation at the twist-4 approximation.

Recently, the predictions of the GLR-MQ equation for the gluon saturation scale were studied in [9]. However, the applications of the AGK cutting rule in the GLR-MQ equation was argued in a more general consideration by two of us (WZ and JHR) in [10], where the Feynman diagrams are summed in a quantum field theory framework instead of the AGK cutting rule. We shall refer to this evolution equation as the MD-DGLAP equation. A major difference among the above mentioned nonlinear equations is that the momentum conservation is restored in the MD-DGLAP equation by the antishadowing corrections,

which may change the predictions of the GLR-MQ equations.

The purpose of this work is to study the behavior of the parton (quark and gluon) distributions in Q^2 and x at high gluon density using the MD-DGLAP equation. It is know that the solutions of QCD evolution equations are sensitive to the input parton distributions. Works [9] use the CTEQ input distributions [11] at $Q_0^2 = 1.4 GeV^2$ to fit the HERA data for the structure function $F_2(x, Q^2)$ of proton. Then they predict the saturation scales Q_s^2 in proton and nucleus by evolving backward from a higher Q^2 scale, where the nonlinear terms in the equation can be neglected. Therefore, one can linearly add the input distributions of the nucleons in a nuclear target. However, the backward evolution paths for gluon and sea quarks are not unique and hence there are uncertainties in the results. Different from works [9], we use the GRV model [12] for input distributions, where the evolution begins in a very low $Q_0^2 < 1 \ GeV^2$. All partons in the GRV input take the valence-like form and it implies the finiteness of parton number and low density of partons. Therefore, we can construct the input distributions in the nucleus using the input set for proton and evolve them according to the standard evolution technique.

We fit the parameters in the input distributions using the HERA data [13] for both $F_2(x, Q^2)$ and $dF_2(x, Q^2)/d\ln Q^2$ in proton in a limiting kinematical region. Then we predict the small x behaviors of parton distributions at different scale Q^2 in proton and nucleus, respectively. We find obvious screening effects in quark and gluon distributions. We also show that a partial saturation appears in the parton distributions of proton. In particular, a flatter plateau appears in the region of smaller x and lower Q^2 in middle and heavy nuclei. However, we have not found the saturation scale Q_s^2 in the expected domain according to the definition in literatures [5,14]. We introduce the new scales Q_R^2 and x_s to describe the small x behaviors of parton distributions in the leading recombination region. We also study the contributions of the antishadowing terms in the MD-DGLAP

equation. Antishadowing compensates the lost momentum in shadowing. Although this lost momentum is little, our calculations show that the contributions of the antishadowing terms to the saturation phenomena can not be neglected.

The paper is organized as follows. In section 2 we introduce the MD-DGLAP equation and compare it with the GLR-MQ equation. In section 3 we fit the parameters in the GRV-like input distributions in the proton using the MD-DGLAP equation and HERA data, then we predict the parton distributions beyond the HERA region. In section 4 we discuss the parton distributions in the nucleus. The discussions and a summary are given in section 5.

2 The MD-DGLAP equation

As we know that the DGLAP equation produces a rapid growth of gluon density toward smaller values of x. The gluons therefore must begin to spatially overlap and recombine in a thin target disc. In works [10], the corrections of parton recombination to the QCD evolution equation are considered by summing up all possible twist-4 cut diagrams in the LLA(Q^2). In the derivation of the equation, the time-ordered perturbation theory instead of the AGK cutting rule is used to pick up the contributions of the leading recombination diagrams. In consequence, the corrections of the gluon recombination to the evolution of parton distributions with Q^2 are described by the following modified DGLAP equation [10]

$$\frac{dxG(x, Q^2)}{d \ln Q^2}$$

$$= P_{gg}^{AP} \otimes G(x, Q^2) + P_{gq}^{AP} \otimes S(x, Q^2)$$

$$+ \frac{\alpha_s^2 K}{Q^2} \int_{x/2}^{x} dx_1 x x_1 G^2(x_1, Q^2) \sum_i P_i^{gg \to g}(x_1, x)$$

$$- \frac{\alpha_s^2 K}{Q^2} \int_{x}^{1/2} dx_1 x x_1 G^2(x_1, Q^2) \sum_i P_i^{gg \to g}(x_1, x) \tag{1a}$$

for gluon distribution and

$$\frac{dxS(x, Q^2)}{d \ln Q^2}$$

$$= P_{qg}^{AP} \otimes G(x, Q^2) + P_{qq}^{AP} \otimes S(x, Q^2)$$

$$+ \frac{\alpha_s^2 K}{Q^2} \int_{x/2}^{x} dx_1 x x_1 G^2(x_1, Q^2) \sum_i P_i^{gg \to q}(x_1, x)$$

$$- \frac{\alpha_s^2 K}{Q^2} \int_{x}^{1/2} dx_1 x x_1 G^2(x_1, Q^2) \sum_i P_i^{gg \to q}(x_1, x) \tag{1b}$$

for sea quark distributions, where P^{AP} are the evolution kernels of the linear DGLAP equation and the recombination functions

$$\sum_i P_i^{gg \to g}(x_1, x)$$

$$= \frac{27}{64} \frac{(2x_1 - x)(-136xx_1^3 - 64x_1x^3 + 132x_1^2x^2 + 99x_1^4 + 16x^4)}{xx_1^5},$$

(1c)

and

$$\sum_i P_i^{gg \to q}(x_1, x)$$

$$= \frac{1}{48} \frac{(2x_1 - x)(36x_1^3 + 49x_1x^2 - 14x^3 - 60x^2x)}{x_1^5}.$$

(1d)

The nonlinear coefficient K in Eq. (1) depends on the definition of double parton distribution and the geometric distributions of partons inside target. For simplicity, we take K as a free parameter in this work. Comparing with the GLR-MQ equation [6]:

$$\frac{dxS(x, Q^2)}{d\ln Q^2}$$

$$= P_{qg}^{AP} \otimes G(x, Q^2) + P_{qq}^{AP} \otimes S(x, Q^2)$$

$$- \frac{1}{30} \frac{\alpha_s^2 K_{GLR-MQ}}{Q^2} [xG(x, Q^2)]^2 + ... + G_{HT},$$

(2a)

and

$$\frac{dxG(x, Q^2)}{d\ln Q^2} = P_{gg}^{AP} \otimes G(x, Q^2) + P_{gq}^{AP} \otimes S(x, Q^2)$$

$$- \frac{\alpha_s^2 K_{GLR-MQ}}{Q^2} \int_x^{1/2} \frac{dx_1}{x_1} [x_1 G(x_1, Q^2)]^2,$$

(2b)

there are following properties in Eq. (1):

(i) The third term on the right-hand side of Eq. (1) is positive and it is called as the antishadowing, while the negative fourth term arises from the shadowing correction. The coexistence of shadowing and antishadowing in the QCD evolution of the parton densities is a general requisition of the local momentum conservation. We emphasize that the

shadowing and antishadowing terms are defined on different kinematics domains $[x, 1/2]$ and $[x/2, x]$, respectively. Thus, the net recombination effects in Eq. (1) are not only related to the value of gluon density, but also depend on the slope of the gluon distribution in the space $[x/2, x]$, i.e., a steeper (or flatter) gluon distribution has a stronger (or weaker) antishadowing effect. On the other hand, the AGK cutting rule is used in the derivation of Eq. (2) and where it is assumed that both the positive and negative contributions of the Feynman diagrams have the same kinematics domain. This results in the violation of the momentum conservation in the GLR-MQ equation.

(ii) The GLR-MQ equation (2) takes the double leading logarithmic approximation (DLLA) for both Q^2 and $1/z$, where one keeps only the $\ln(Q^2/\mu^2)\ln(1/z)$ factor in the solutions of the evolution equation or, equivalently, takes only the terms having $1/z = x_1/x$ factor. On the other hand, the MD-DGLAP equation (1) is derived under the leading logarithmic approximation for Q^2. Therefore, Eqs. (1c) and (1d) contain the terms beyond the leading $1/z$ approximation. One can find that the contributions from these terms do not vanish even in the small x region, since z runs from x to 1 as x_1 varies, that is z is not restricted in a smaller-z region.

(iii) Note that the sea quark evolution in Eqs. (1) and (2) take different forms. The reason is that the transition of gluon→ quarks is suppressed in the DLLA-manner. The DLLA diagram only contains the gluon ladders and any transitions of gluon → quark break the gluon ladder-structure. Therefore, a special technique is used to include the corrections of gluon recombination to the quark distributions in the GLR-MQ equation. However, this extra technique is unnecessary in the derivation of the MD-DGLAP equation, since we can produce the evolution equations for gluon and sea quarks in a same framework at the $LLA(Q^2)$.

Therefore, we use the MD-DGLAP equation to study the saturation phenomena in-

stead of the GLR-MQ dynamics. We shall show the different predictions of the evolution

equations with or without antishadowing terms in Sec. 5.

3   The solutions of the MD-DGLAP equation in proton

The numerical solutions of evolution equation depend sensitively on the input parton (gluon and quark) distributions at a lower scale Q_0^2. In principle, they are not calculable within perturbative QCD but are determined by data. Because the electromagnetic probe can not directly measure the gluon density, the input gluon distribution has a larger uncertainty. The early data for the DIS structure functions can always be fitted by using the linear DGLAP equation provided that a satisfying input gluon density is assumed. However, new HERA data in small x region, in particular the slopes of the structure function $dF_2/d\ln Q^2$ have restricted the above mentioned uncertainty. In fact, the global analysis of the HERA data using the DGLAP dynamics are given by the MRST [15] and CTEQ [11] collaborations. Where a MRST2001 set shows the negative value of gluon distribution in $Q^2 < 1GeV^2$. It means that if a positive input gluon distribution below 1 GeV^2 is taken, the screening corrections to the evolution equation are useful.

In this work, we use the GRV-like input distributions. In the GRV model [12], the parton distributions are evolved from a very lower resolution scale (but larger than the QCD parameter Λ_{QCD}). A specific assumption of the GRV model is that the input parton distributions take the simple valence-like distribution form. The GRV model with the linear DGLAP evolution equation gives a good description for proton structure function $F_2(x, Q^2)$ in a broad region but the fit in the slope of $F_2(x, Q^2)$ at lower Q^2 remains to be improved (see the dashed curves in Fig. 2). We shall show that the corrections of the gluon recombination improved the fit. In practice, we use the initial valence quark- and gluon-densities in the GRV98LO set [16] as the input distributions at $Q_0^2 = 0.34GeV^2$, i.e.,

$$xU(x, Q_0^2) = 1.239x^{0.48}(1-x)^{2.72}(1-1.8\sqrt{x}+9.5x),$$

$$xD(x, Q_0^2) = 0.614(1-x)^{0.9}xU(x, Q_0^2),$$

and

$$xG(x, Q_0^2) = 17.47x^{1.6}(1-x)^{3.8}, \tag{3}$$

and the mass of charm quark is 1.4 GeV. In the meantime, we let the parameters in the sea quarks distributions to be determined by the HERA data [13] in the MD-DGLAP evolution equation. The results are

$$x(\bar{d}(x, Q_0^2) + \bar{u}(x, Q_0^2)) = 0.9x^{0.01}(1-x)^{8.0}(1-3.6\sqrt{x}+7.8x),$$

$$x(\bar{d}(x, Q_0^2) - \bar{u}(x, Q_0^2)) = 0.23x^{0.48}(1-x)^{11.3}(1-12.0\sqrt{x}+50.9x). \tag{4}$$

In this fit, the nonlinear coefficient K in the evolution equation is taken as $K = 0.0014$. It implies that the nonlinear recombination corrections can not be neglected in the HERA data [13]. The results are shown in Figs. 1 and 2 (solid curves), where the dashed lines are the fitting results of the linear DGLAP equation using the GRV98LO [16] as the input distributions. One can find that the contributions of gluon recombination improve the fit in $Q^2 > 1GeV^2$. There are derivations between the fit and data in $Q^2 < 1GeV^2$, they imply that the corrections of beyond LLA(Q^2) are necessary at very lower Q^2. However, as we shall show that our main conclusions in this work are insensitive to the choices of parameters in the GRV-like input.

Now we give the predictions of the gluon and quark distributions beyond HERA region in Figs. 3-6 (solid curves). The parton distributions from the DGLAP equation with GRV98LO are also plotted (dashed curves) for comparison. The results show obvious

suppression in both the quark and gluon distributions and a flat tendency at the small x limit. Figures 5 and 6 give the Q^2-dependence of parton distributions at fixed values of x. The dashed curves (the predictions of the DGLAP dynamics) in Figs. 3 and 4 have the exponential form ($\sim \exp[\sqrt{\ln 1/x}]$) and it violates the unitarity. However, the solid curves (the results of the MD-DGLAP equation) show that the growth of $xG(x, Q^2)$ and $xS(x, Q^2)$ is slower than $\ln(1/x)$ in $1 < Q^2 < 10 GeV^2$ and $x < 10^{-6}$. This partial saturation behavior is softer than the predicted result by the DGLAP equation and the BFKL equation ($\sim x^{-\lambda}$, $\lambda > 0$).

In hadron-hadron cross section, such as p-p, the Froissart boundary [17] requires

$$\sigma^{pp}(s) \leq \frac{\pi}{m_\pi^2} log^2(s/s_0), \tag{5}$$

at the high s limit, where s is the center-of-mass energy squared and $x = Q^2/s$. The high energy limit implies the small x approximation when Q^2 is fixed to be a few GeV^2. Therefore, although the gluon- and quark-distributions in proton do not saturate at small values of x, but their partial saturation-behavior satisfies the Froissart boundary in the perturbative QCD means.

As we know that the saturation scale $Q_s^2(x)$, which indicates the saturation limit, is usually defined [5, 14] to be

$$\frac{dxG(x, Q^2)}{d \ln Q^2}\Big|_{Q_s^2} = 0, \tag{6a}$$

and

$$\frac{dxS(x, Q^2)}{d \ln Q^2}\Big|_{Q_s^2} = 0, \tag{6b}$$

or equivalently

$$W_s \equiv \frac{nonlinear\ terms\ of\ Eq.(1)}{linear\ terms\ of\ Eq.(1)}\Big|_{Q_s^2} = 1, \tag{7}$$

which requires that the nonlinear recombination effect in the MD-DGLAP equation fully

balances the linear splitting effect. Thus the saturation limit is reached. However, we

have not found such saturation solution Q_s^2 in Eq. (1). It means that the net shadowing

(i.e., shadowing-antishadowing) effect in the leading recombination approximation is not

large enough to cancel the increase of parton densities with increasing Q^2. In other

words, the higher-order recombination contributions would become significant and should

be included in the evolution equation near the saturation limit. However, in this paper

we focus on the range where the gluon recombination begins to work. Therefore, we

introduce the recombination scale $Q_R^2(x)$ instead of $Q_s^2(x)$ as follows:

$$W_R \equiv \frac{nonlinear\ terms\ of\ Eq.(1)}{linear\ terms\ of\ Eq.(1)}\Big|_{Q_R^2} = \alpha_s(Q_R^2(x)). \tag{8}$$

The $Q_R^2(x)$ for the gluon distribution in proton is shown in Fig. 7 (solid curve). It is

interesting that the line has a corner near $Q_R^2(x) \simeq 2GeV^2$. The anomalous behavior of

the line at $Q_R^2(x) \leq 2GeV^2$ is the results of the antishadowing corrections. In fact, the

relative stronger antishadowing effect at lower Q^2 locally raises the gluon distribution.

It shifts the flatter plateau toward a larger x- value. We can also see this effect in the

behaviors of x_s in Figs. 3, 8 and 9 (see following sections).

We can find that the gluon recombination obviously suppresses the evolution of parton

densities in $x < 10^{-6}$ in proton. According to the definition, one can see $Q_R^2(x) < Q_s^2(x)$.

The evolution of the parton distributions from $Q_R^2(x)$ to $Q_s^2(x)$ is a complicated process.

We shall show that the contributions of the leading recombination are also important in

the nuclear target near Q_R^2.

4 The solutions of the MD-DGLAP equation in nucleus

Nuclear target is an ideal laboratory for the research of the saturation phenomena, since the gluon recombination corrections are enhanced due to the correlation of gluons belonging to different nucleons at a same impact in the nuclear target. It is well known that the nuclear shadowing is a complicated phenomenon which has two different sources [18]: (i) it perturbatively originates from gluon recombination in the infinite momentum frame of nuclear target, or from multiple scattering in the target-rest frame; (ii) the non-perturbative nuclear effects. The former is expressed as the nonlinear QCD evolution equations, while the later relates to the structure of the input parton distributions. We have interest in the separate relations of nuclear saturation phenomena with the above mentioned two sources. Therefore, at first step, we neglect the non-perturbative nuclear effects. The gluon distribution (3) implies a small total number and very low density of gluons, where the recombination corrections are negligible. This conclusion can be confirmed from the following Fig. 8, which indicates that the gluon distributions with and without recombination corrections are similar near the evolution start point. Thus, we can predict the nuclear parton densities using the input distributions (3-4) and the MD-DGLAP equation, where the nonlinear terms are multiplied by $A^{1/3}$.

Figures 8-11 and 12-15 are the results corresponding to Figs. 3-6 but for Ca($A = 40$) and Pb($A = 208$), respectively. Our results show the plateau in the parton distributions in $x < 10^{-6}$ and $1 < Q^2 < 10 GeV^2$. We note that in the DGLAP dynamics the generated gluon and sea quark distributions in small x region will speed up transfer from the valence form into the power form also through a plateau. However, this plateau exists in a very narrow Q^2-window and it is unstable. The plateau in Figs. 8-9 and 12-13 implies a saturation behavior in the parton distributions at the small x limit. We use x_s to indicate

this saturation effect and is defined as

$$\frac{dxG(x, Q^2)}{d\ln\frac{1}{x}}\Big|_{x_s} = 0, \qquad (9a)$$

and

$$\frac{dxq(x, Q^2)}{d\ln\frac{1}{x}}\Big|_{x_s} = 0. \qquad (9b)$$

The value of x_s is in windows $10^{-7} < x_s < 10^{-4}$ and $1 < Q^2 < 10 GeV^2$ for the middle and heavy nuclear target. The results show that the antishadowing effect impedes the shift of x_s toward smaller value with increasing Q^2 in the range of $Q^2 < 2 GeV^2$. We can also find that the altitude of the plateau almost grows linearly with increasing Q^2 in Fig. 16. This consists with the geometric scaling [3,4].

The values of Q_R^2 for the nuclear gluon distribution are plotted in Fig. 7 (dashed and dotted curves) using Eq. (8). The behavior of curves near $Q_R^2(x) \simeq 2 GeV^2$ is due to the antishadowing corrections, which locally raise the gluon distribution.

Since the MD-DGLAP equation is based on the collinear factorization scheme and its predictions for the parton distributions are universal and independent of the concrete process, the above mentioned saturation phenomena can be checked up in ultra-relativistic heavy ion collisions such as the rapidity distribution and centrality dependence of particle production.

However, we still have not found the saturation solution Q_s^2 of Eq. (7) in the available nuclear target. Obviously, this conclusion is different from the work [9], which uses the GLR-MQ equation to backward evolve the parton distributions from the input distributions of a free proton at very higher Q^2, where the nonlinear terms are negligible. They give $Q_s^2 \sim 3 - 20 GeV^2$ at $10^{-5} < x < 10^{-2}$ for Pb($A = 208$)[9]. One can understand the above mentioned difference as follows. Comparing the solid curves of Figs. 3 and 12,

we find the gluon density in the nucleus at higher Q^2 is much smaller than that in the proton even if the recombination terms in the evolution equation do not play a role at such higher Q^2. The reason is that the parton distributions at higher Q^2 always remember the recombination effects in their evolution process. Therefore, a larger, but not true, input distribution in the nuclear target predicted a stronger recombination effect in work [9], which may balance the parton splitting effect in the evolution, and give a solution in Eq. (7).

Now we consider the corrections of the non-perturbative nuclear effects in the nuclear input parton distributions. The fact that the structure functions of bound and free nucleons are not equal has been discovered long ago and it is called the EMC effect [19]. However, its dynamics is still an open problem since the several mechanisms dominate the EMC effect. Although there are some models to describe the non-perturbative nuclear shadowing relating to the GRV-input distributions [20,21], they still have a larger uncertainty, particularly in the nuclear gluon distribution. In this case, we take following simplified factors R_S and R_G to describe the contributions of the non-perturbative nuclear shadowing like Ref. [22],

$$S_A(x, Q_0^2) = R_S(x, Q_0^2, A)S(x, Q_0^2), \tag{10}$$

for sea quarks and

$$G_A(x, Q_0^2) = R_G(x, Q_0^2, A)G(x, Q_0^2), \tag{11}$$

for gluon, where

$$R_S(x, Q_0^2, A) = \begin{cases} 1, & x_n < x < 1 \\ 1 - K_S(A^{1/3} - 1)\frac{x_n - x}{x_n - x_A}, & x_A \le x \le x_n \\ 1 - K_S(A^{1/3} - 1), & 0 < x < x_A, \end{cases} \tag{12}$$

and

$$R_G(x, Q_0^2, A) = \begin{cases} 1, & x_n < x < 1 \\ 1 - K_G(A^{1/3} - 1)\frac{x_n - x}{x_n - x_A}, & x_A \le x \le x_n \\ 1 - K_G(A^{1/3} - 1), & 0 < x < x_A, \end{cases} \qquad (13)$$

in which $x_n = 0.05$, $x_A = 0.017A^{-1/3}$, and $K_S = 0.09$ are parameterized using the data about the EMC effect [19]; while we take $K_G = K_S$ for the moment. In the meantime, we neglect the EMC effects in $x > 0.05$ since we focus the behavior of parton distributions at very small x limit. Using Eqs. (10)-(13) as the input distributions we evolve the MD-DGLAP equation. Our results are shown in Figs. 17-19 for Ca($A = 40$) and Pb($A = 208$). Comparing these results with Eqs. 7-9, we find that the differences between them are small.

Since we have not enough data to fix the value of K_G, we take the parton distributions for Pb($A = 208$) as an example and change K_G from 0.18 to 0 to test the sensitivity to such choices. We find that the results are insensitive to the above mentioned change since the gluon distribution Eq. (3) in $x < 0.05$ is very small.

Now we can conclude that the saturation- or partial saturation phenomena in the small x behavior of parton distributions are dominated by QCD dynamics rather than non-perturbative nuclear shadowing corrections in the input distributions.

5 Discussions and summary

Let us discuss the antishadowing contributions. Part of momentum is lost due to the negative shadowing terms in the GLR-MQ equation. Most works do not make an attempt to correct the evolution equation from the momentum conservation since the lost momentum is only a few percent of the total momentum. However, as one of us (WZ) has pointed out that the antishadowing contributions, which balance the lost momentum in the shadowing effect can not be neglected [23]. For illustrating this point, we set the antishadowing terms to zero in the MD-DGLAP equation (1) and use it to evolve the parton distributions. In this case, we re-fit the input distributions (4) and take $K = 0.000285$ using the HERA data [13]. New parton distributions in proton, $Ca(A = 40)$ and $Pb(A = 208)$ are plotted by dotted curves in Figs. 3-4, 8-9 and 12-13, respectively. There are following two distinguishing features as compared with solid curves:

(1) The results show that the parton distributions with antishadowing effect are lower than that without antishadowing effect. One can understand the above-mentioned results as follows. The main HERA data, which are used to fit the nonlinear parameter K have shown the steeper form at $Q^2 > 1GeV^2$ and $x > 10^{-4}$, where the antishadowing correction is larger. Therefore, to fit the same HERA data, the value of K in the evolution equation with the antishadowing terms should be larger than that in the evolution equation without the antishadowing terms, since in the former case an obvious antishadowing effect partly cancels the shadowing effect. On the other hand, the net screening effect flats the gluon distribution when x enters into a smaller x region and therefore weakens the antishadowing effect. Therefore, a more stronger net screening effect appeared in Eq. (1). Comparing the solid curves with the dotted curves in Figs. 3 and 4, one can understand that the antishadowing corrections make the growth of the solid curves slower than that of the dotted curves.

The above mentioned differences between the effects with antishadowing and without antishadowing also appear in the predictions of the MD-DGLAP equation (with antishadowing) and the GLR-MQ equation (without antishadowing). Using the same program as we used in the MD-DGLAP equation, we fit the relating parameters in the GLR-MQ equation when using the GRV-like input parton distributions. Then we predict the parton distributions in proton and Pb($A = 208$) (see Figs. 20 and 21). The results show that the screening effect in the GLR-MQ equation is weaker than the net-screening effect in the MD-DGLAP equation if we use similar input parton distributions. Although the plateau has appeared in the parton distributions of Pb($A = 208$), we still have not found saturation solution Q_s^2 in Eq. (6) for the GLR-MQ equation.

(2) An other interesting difference between the predictions of the equations without and with antishadowing corrections is the position of x_s. In the former case x_s always moves toward smaller value with increasing Q^2 (note that x_s runs out the diagrams, for example, at $Q^2 \geq 2GeV^2$ in Fig. 12), while in the later case this shift is impeded by the antishadowing effect in the range of lower Q^2 ($Q^2 < 2GeV^2$). This phenomenon relates to Fig. 7, where the line has a corner near $Q_R^2(x) \simeq 2GeV^2$ due to the relative stronger antishadowing effect at lower Q^2 locally raises the gluon distribution.

As we know that the nuclear shadowing has different manifestations: the suppression in the usual or unintegrated parton distributions and their evolutions, the reduction of the structure functions and the screening effect in the cross sections. There are many different kinds of model to study the above mentioned shadowing phenomena. In this work we do not try to compare the modified DGLAP equations with other versions of the saturation model such as the JIMWLK equation [4]. The reason is that they have different research subjects: the former case discusses the shadowing in the parton distributions, which are independent of the process, while the later case treats the unintegrated parton

distributions and the cross sections, which are process-dependent.

Finally, we take the LLA(Q^2) in this work. The contributions beyond the LLA(Q^2) are necessary for the improvement of predictions in the range of very lower Q^2 ($Q^2 < 1 GeV^2$). However, it relates to the further study including the evolution dynamics at higher order.

In summary, the parton distributions in small x region are numerically predicted by using a modified DGLAP equation with the GRV-like input distributions. We show that the gluon recombination at twist-4 level obviously suppresses the rapid growth of parton densities with x decrease. The growth of predicted parton distributions in proton towards small x is slower than $\ln(1/x)$ in $x < 10^{-6}$. In particular, a plateau is formed in the parton distributions of the nuclear target at small x limit and $1 < Q^2 < 10 GeV^2$. The altitude of the plateau almost grows linearly with Q^2 increasing, i.e., the geometrical scaling. Thus, the parton distributions in proton and nucleus unitarize, and the Froissart boundary is not violated in the asymptotic regime of high density QCD. The saturation (or partial saturation) phenomena appear before the saturation scale Q_s^2, where the gluon recombination correction fully balance the parton splitting effects. The predicted saturation phenomena can be checked up in ultra-relativistic heavy ion collisions such as the rapidity distribution and centrality dependence of particle production.

Acknowledgments:

References

[1] G. Altarelli and G. Parisi, Nucl. Phys. B126, 298 (1977); V.N. Gribov and L.N. Lipatov, Sov. J. Nucl. Phys. 15, 438, 675 (1972); Yu.L. Dokshitzer, Sov. Phys. JETP. 46, 641 (1977).

[2] L.N. Lipatov, Sov. J. Nucl. Phys. 23, 338 (1976); V. S. Fadin, E.A. Kuraev and L.N. Lipatov, Phys. Lett. B 60, 50 (1975); E.A. Kuraev, L.N. Lipatov and V. S. Fadin, Sov. Phys. JETP 44, 443 (1976); E.A. Kuraev, L.N. Lipatov and V. S. Fadin, Sov. Phys. JETP 45, 199 (1977); I. I. Balitsky and L.N. Lipatov, Sov. J. Nucl. Phys. 28, 822 (1978); I. I. Balitsky and L.N. Lipatov, JETP Lett. 30, 355 (1979).

[3] For a review, see A.H. Mueller, arXiv:hep-ph/0111244, and references therein, as well as

[4] E. Iancu, A. Leonidov and L. McLerran, arXiv:hep-ph/0202270, and references therein.

[5] L.V. Gribov, E.M. Levin and M.G. Ryskin, Phys. Rep. **100**, 1 (1983).

[6] A.H. Mueller and J. Qiu, Nucl. Phys. **B268**, 427 (1986).

[7] V.A. Abramovsky, J.N. Gribov and O.V. Kancheli, Sov. J. Nucl. Phys. **18**, 593 (1973).

[8] A.H.Mueller, Nucl.Phys. **B415**, 373 (1994) ; **B437**, 107 (1995).

[9] K.J. Eskola, H. Honkanen, V.J. Kolhinen, Jianwei Qiu, C.A. Salgado, Nucl.Phys. **B660**, 211 (2003) [arXiv:hep-ph/0211239]; arXiv:hep-ph/0302185.

[10] W. Zhu, Nucl. Phys. **B551**, 245 (1999) [arXiv:hep-ph/9809391]; W. Zhu and J.H. Ruan, Nucl. Phys. **B559**, 378 (1999) [arXiv:hep-ph/9907330].

[11] H. L. Lai et al. [CTEQ Collaboration], Eur. Phys. J. **C12**, 375 (2000) [arXiv:hep-ph/9903282].

[12] M. Glück, E.Reya and A. Vogt, Z. Phys. **C48**, 471 (1990).

[13] C. Adloff et al. [H1 Collaboration], Nucl. Phys. **B497**, 3 (1996); Eur. Phys. J. **C21**, 33 (2001); J. Breitweg et al. [ZEUS collaboration], Eur. Phy. J. **C7**, 3 (1999); Phys. Lett. **B487**, 53 (2000); Eur. Phy. J. **C21**, 443 (2001).

[14] J. Kwiecinski, A.D. Martin, W.J. Stiring and R.G. Roberts, Phys. Rev. **D42**, 3645 (1990), and references therein.

[15] A. D. Martin, R. G. Roberts, W. J. Stirling and R. S. Thorne, Eur. Phys. J. **C23**, 73 (2002) [arXiv:hep-ph/0110215]; A. D. Martin, R. G. Roberts, W. J. Stirling and R. S. Thorne, Phys. Lett. **B531**, 216 (2002) [arXiv:hep-ph/0201127].

[16] M. Glück, E. Reya and A. Vogt, Eur. Phys. J. **C5**, 461 (1998).

[17] M. Froissart, Phys. Rev. 123, 1053 (1961); L. Lukaszuk and A Martin, Il Nuovo Cimento **47A**, 265 (1967).

[18] G. Piller, W. Weise, Phys. Rep. **330**, 1 (2000).

[19] M. Arneodo, Phys. Rep. **240**, 301 (1994).

[20] D.Indumathi and W. Zhu Z. Phys. **C74**, 119 (1997).

[21] K.J. Eskola, V.J. Kolhinen and C.A. Salgado, Eur. Phys. J. **C9**, 61 (1999).

[22] J. Qiu, Nucl. Phys. **B291**, 746 (1987).

[23] W. Zhu, D.L. Xu, K.M. Chai and Z.X. Xu, Phys. lett. **B317**, 320 (1993); W. Zhu, K.M. Chai and B. He, Nucl. Phys. **B427**, 525 (1994), **B449**, 183 (1995).

Figure Captions

Fig. 1 The fits of the computed $F_2(x, Q^2)$ in proton by the MD-DGLAP equation (solid curves) to (a) H1- and (b) ZEUS-data. The dashed curves are the DGLAP equation results from GRV98LO.

Fig. 2 The fits of the computed $dF_2(x, Q^2)/d\ln Q^2$ in proton by the MD-DGLAP equation (solid curves) to the H1 data,. The dashed curves are the DGLAP equation results from GRV98LO.

Fig. 3 The predictions for the gluon distribution function in proton. The solid (dotted) curves are the results of the MD-DGLAP equation with (without) antishadowing corrections; The dashed curves are the results of the DGLAP equation with the GRV98LO. Notice that the solid and dashed curves have opposite concavities.

Fig. 4 As Fig. 3 but for the sea-quark distribution function in proton.

Fig. 5 The Q^2-dependence of the gluon distribution function in proton at fixed values of x, the solid (dotted) curves correspond to with (without) antishadowing contributions. The dashed curves are the results of the DGLAP equation.

Fig. 6 As Fig. 5 but for the sea-quark distribution function in proton.

Fig. 7 The gluon recombination scale $Q_R^2(x)$ in the MD-DGLAP equation for proton (solid curve), Ca($A = 40$) (dotted curve) and Pb($A = 208$) (dashed curve); where the input distributions are Eqs. (3) and (4).

Fig. 8 The predictions for the gluon distribution function in Ca($A = 40$). The solid (dotted) curves are the results of the MD-DGLAP equation with (without) antishadowing contributions; The dashed curves are the results of the DGLAP equation; where the input distributions are Eqs. (3) and (4).

Fig. 9 As Fig. 8 but for the sea-quark distribution function.

Fig.10 The Q^2 dependence of the gluon distribution function in Ca($A = 40$) at fixed

values of x, from with (solid curves) and without (dotted curves) antishadowing corrections in the present work. The dashed curves are the results of the DGLAP equation. Notice the plateau at small x; where the input distributions are Eqs. (3) and (4). .

Fig. 11 As Fig. 10 but for the sea-quark distribution function.

Fig. 12 As Fig. 8 but for $Pb(A = 208)$.

Fig. 13 As Fig. 9 but for $Pb(A = 208)$.

Fig. 14 As Fig. 10 but for $Pb(A = 208)$.

Fig. 15 As Fig. 11 but for $Pb(A = 208)$.

Fig. 16 Parts of Figs. 14 and 15. The lines show that the altitude of the plateau in $Ca(A = 40)$ and $Pb(A = 208)$ almost grows linearly with increasing Q^2.

Fig. 17 The predictions for the gluon distribution function in $Ca(A = 40)$ and $Pb(A = 208)$ using the MD-GDLAP equation and input distributions Eqs. (10)-(13).

Fig. 18 The predictions for the quark distribution functions in $Ca(A = 40)$ and $Pb(A = 208)$ using the MD-GDLAP equation and input distributions Eqs. (10)-(13).

Fig. 19 As Fig. 7 but the input distributions are taken as Eqs. (10)-(13).

Fig. 20 The predictions for the gluon distribution function using the GLR-MQ evolution equation with a GRV-like input parton distributions. The solid and dotted curves are the results in proton and $Pb(A = 208)$.

Fig. 21 As Fig. 20 but for the sea-quark distribution function.
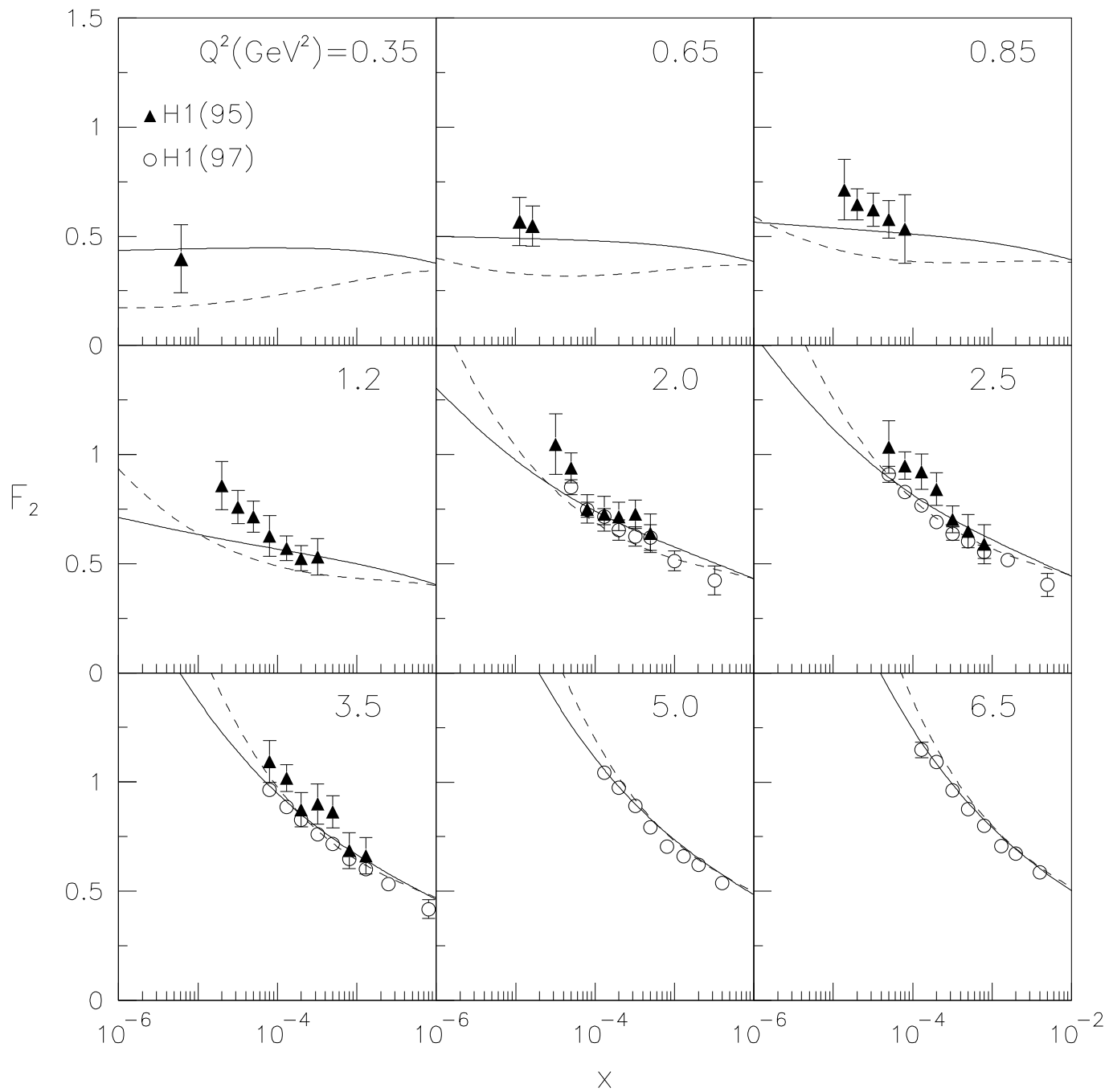
Fig.1(a)
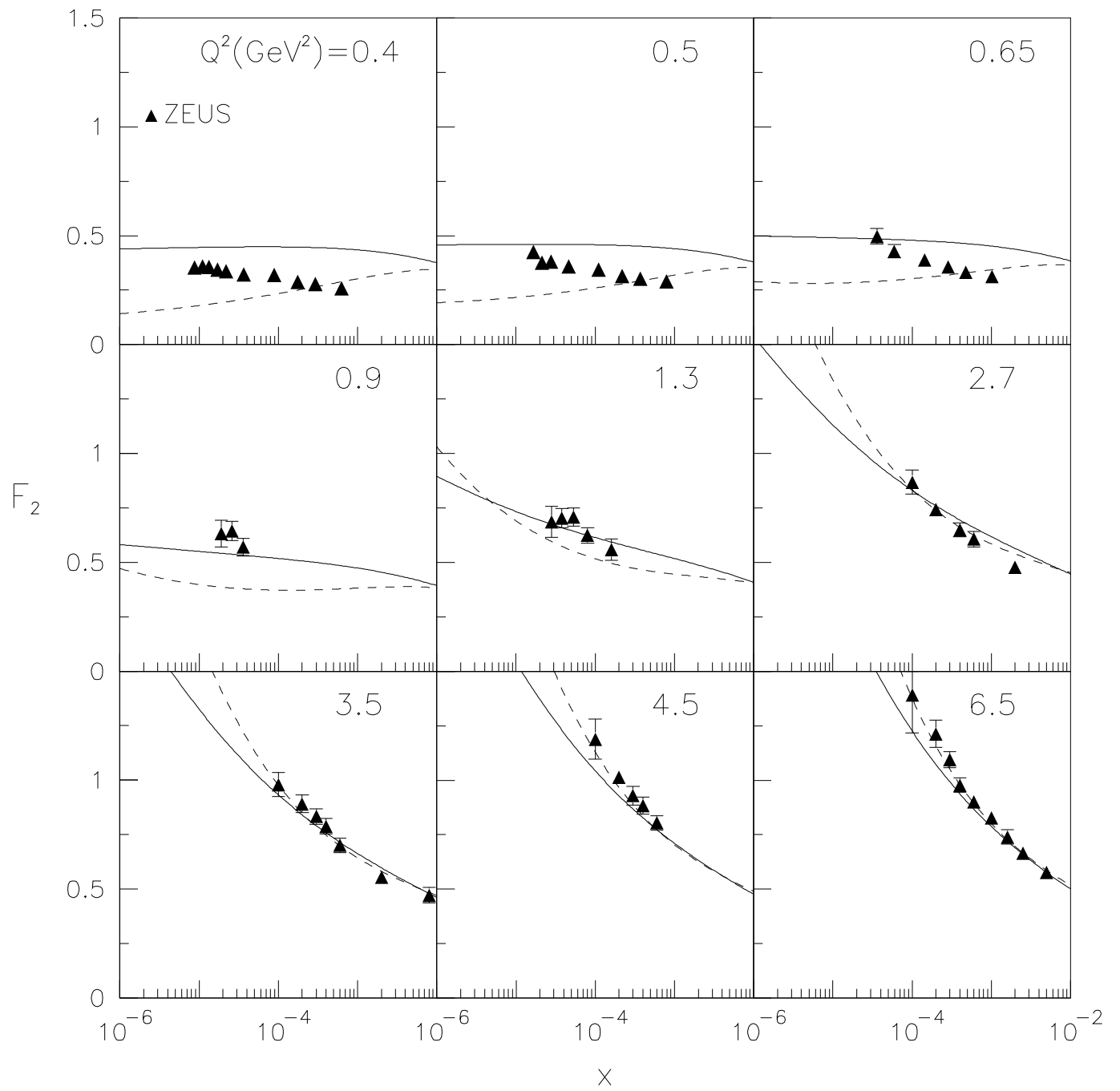
Fig.1(b)
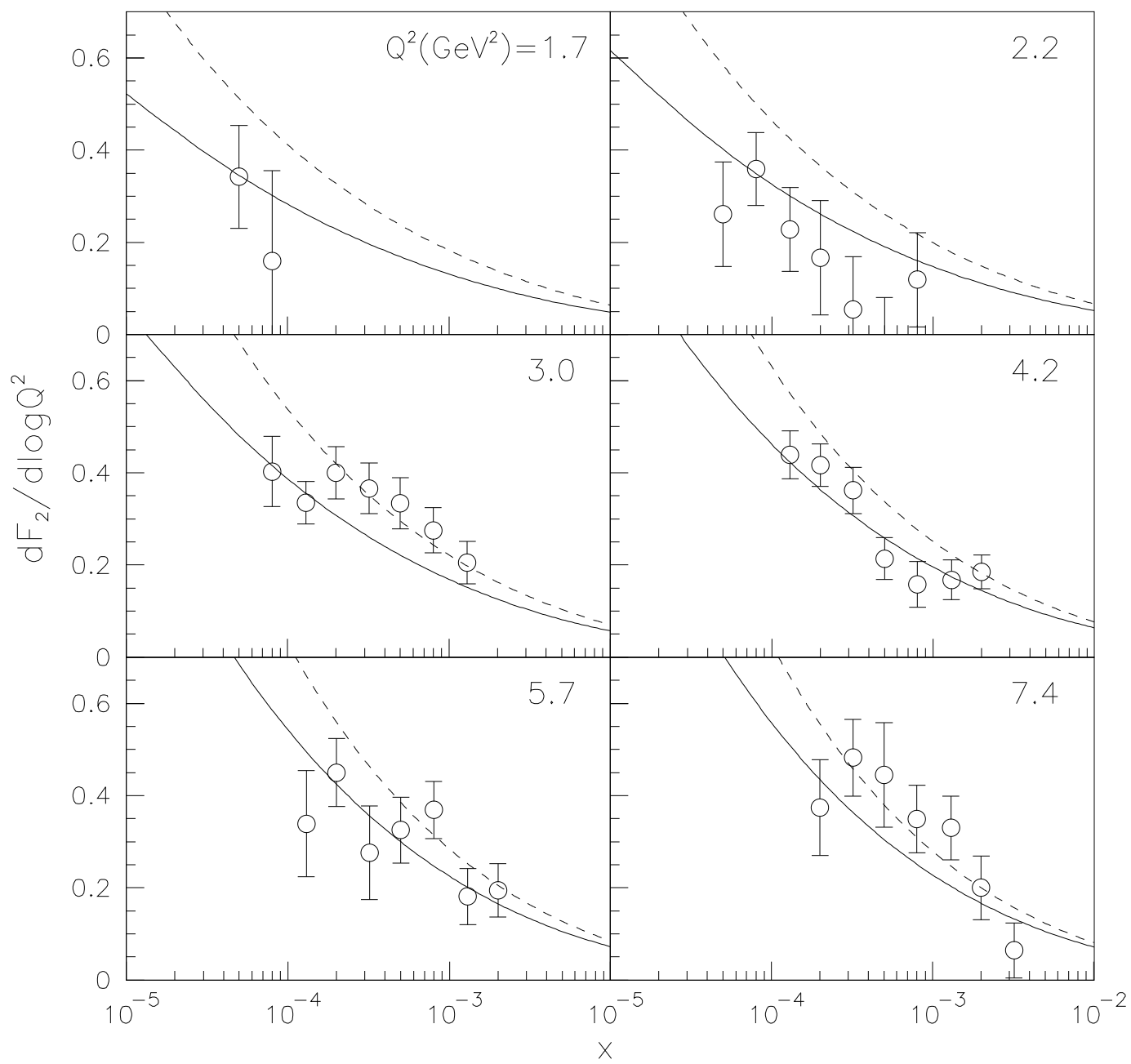
Fig.2
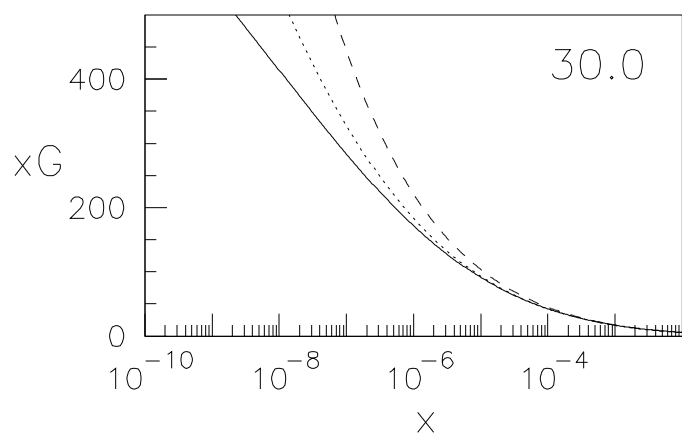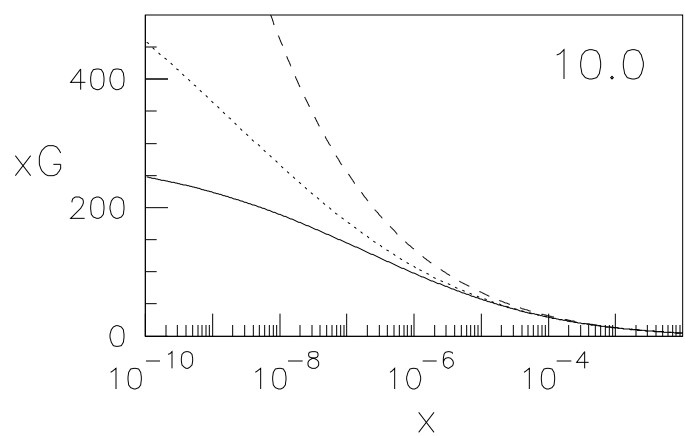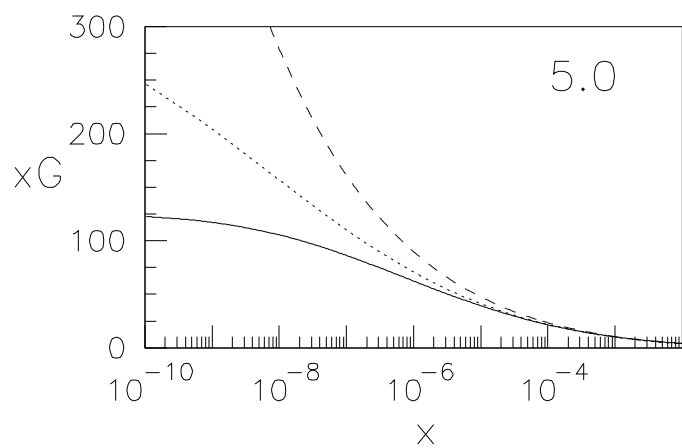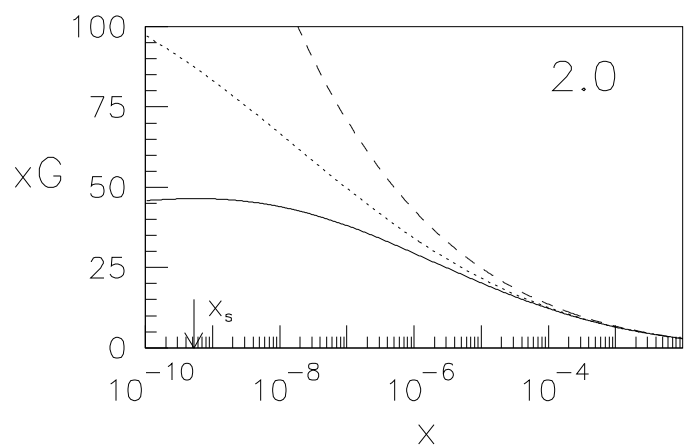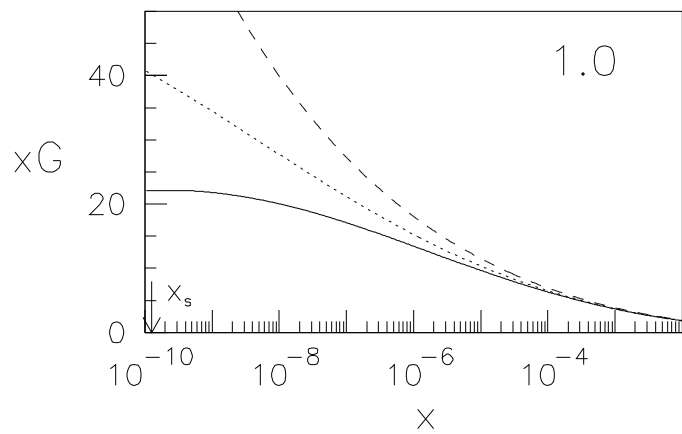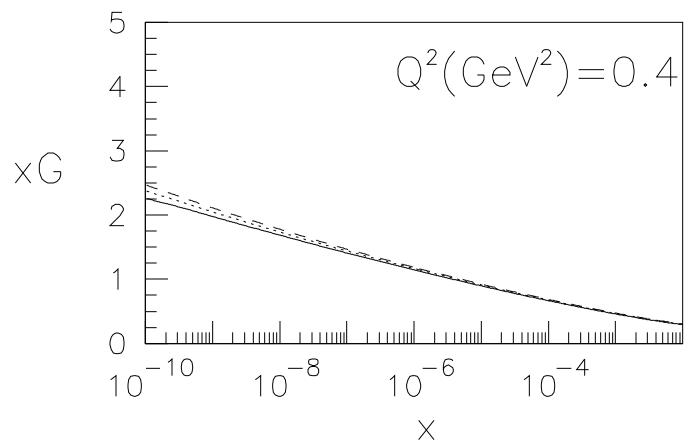
Fig.3
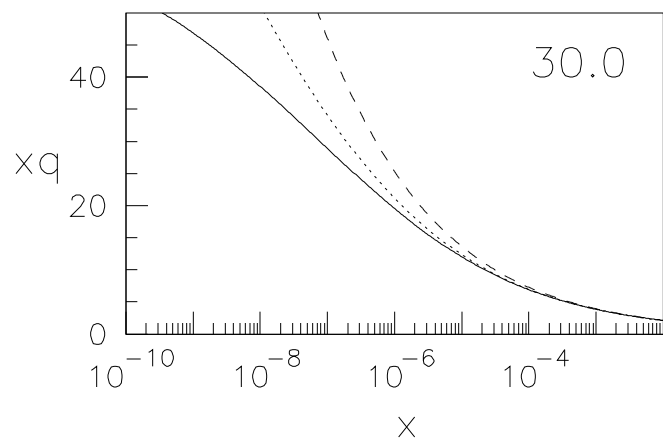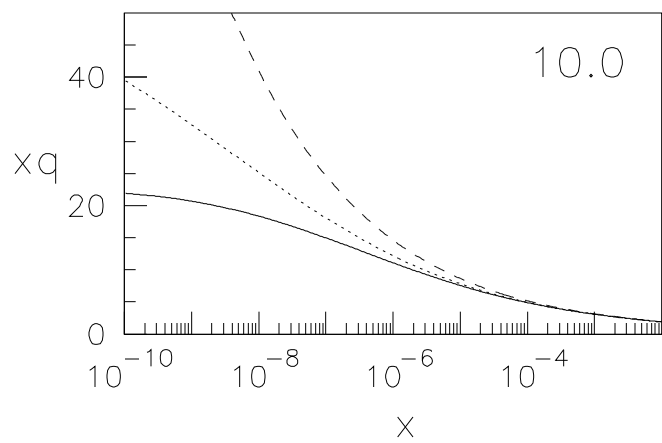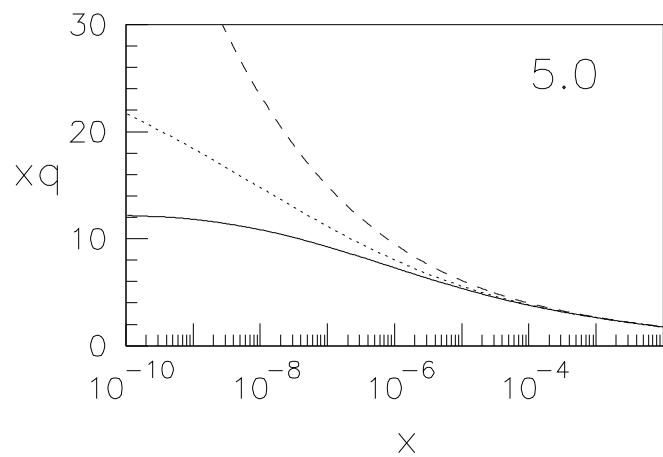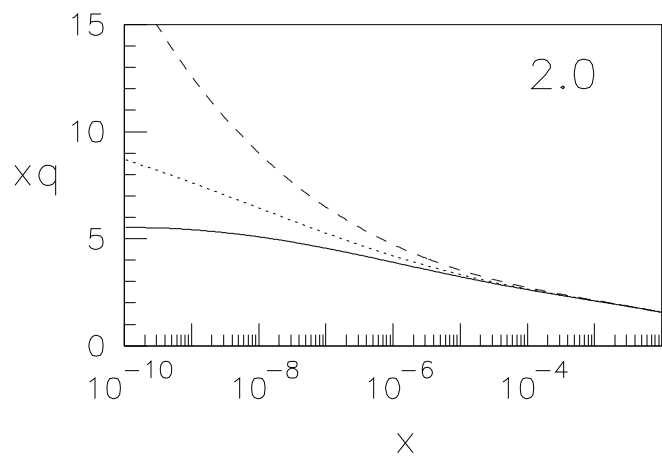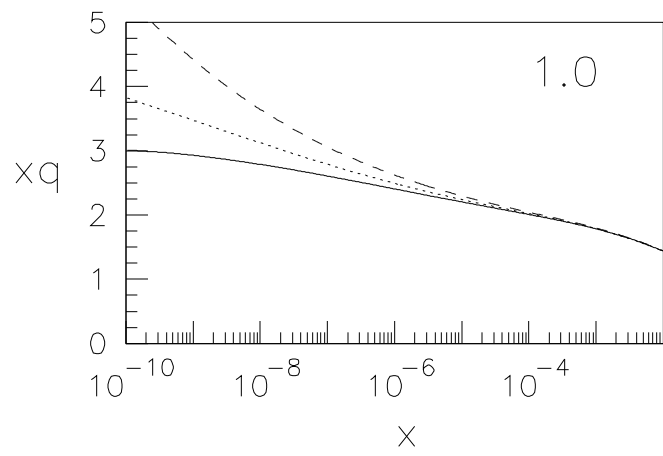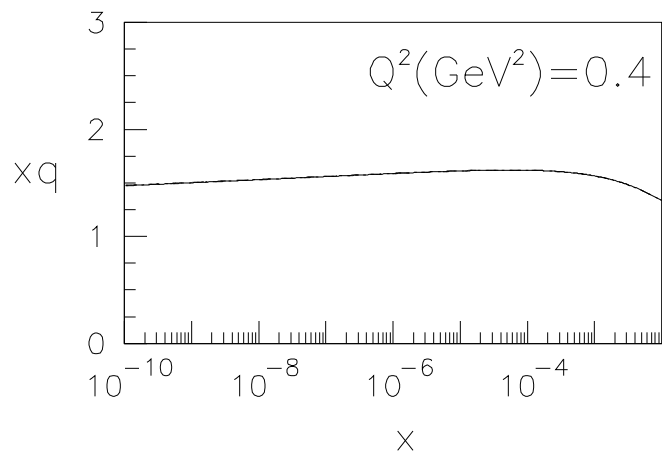
Fig.4
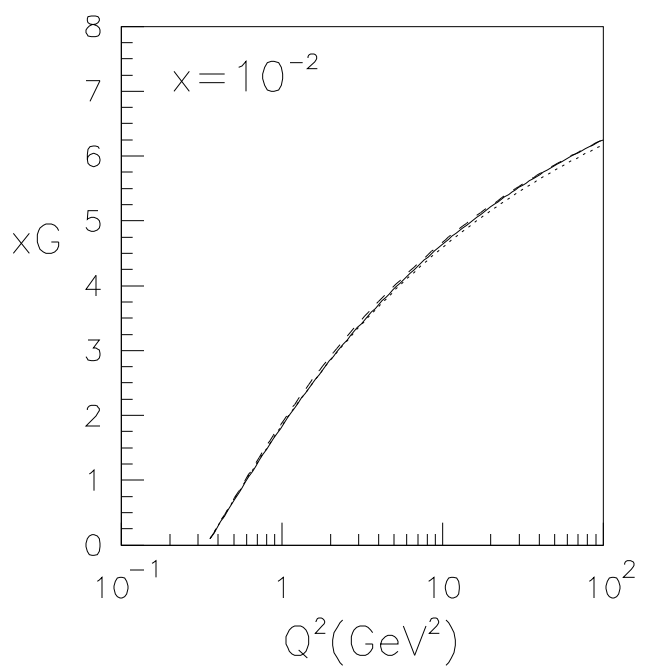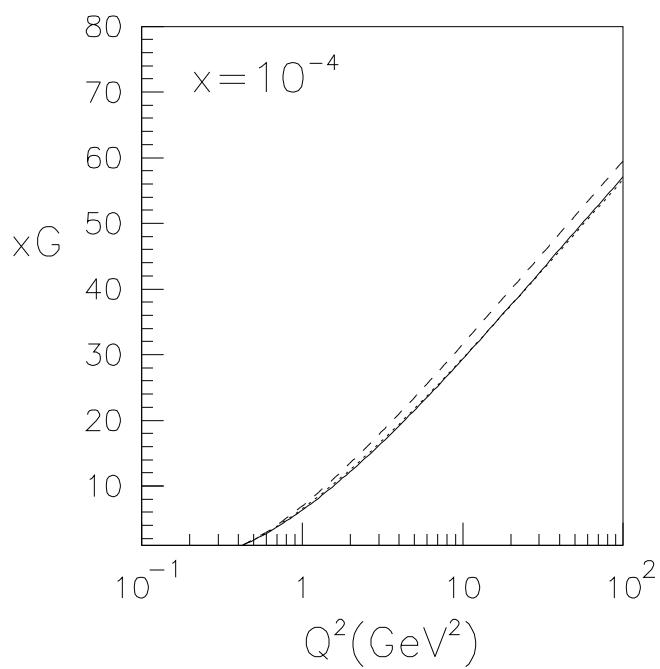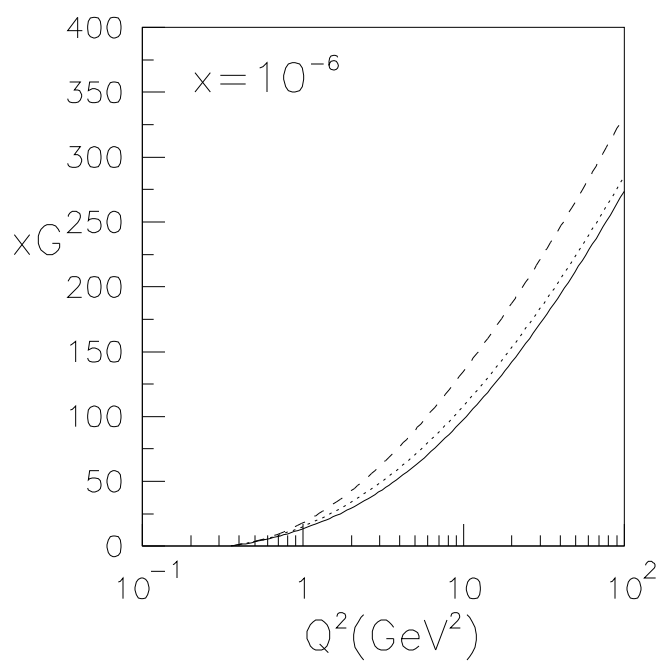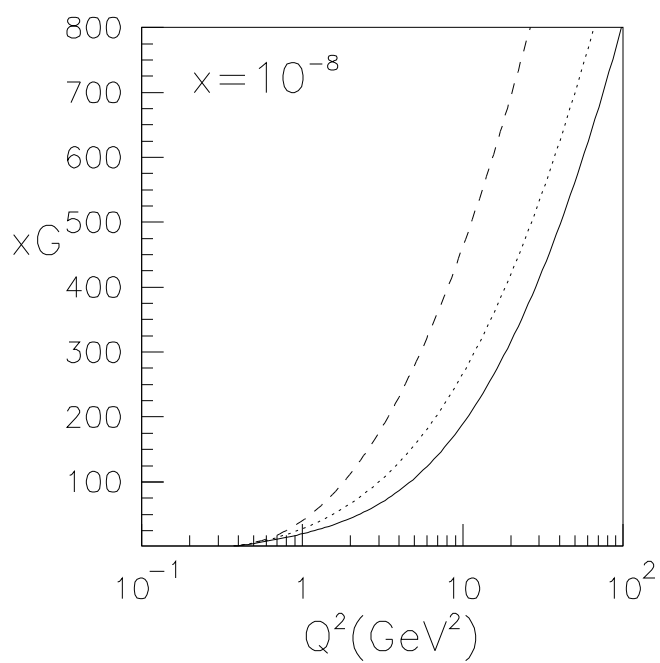
Fig.5
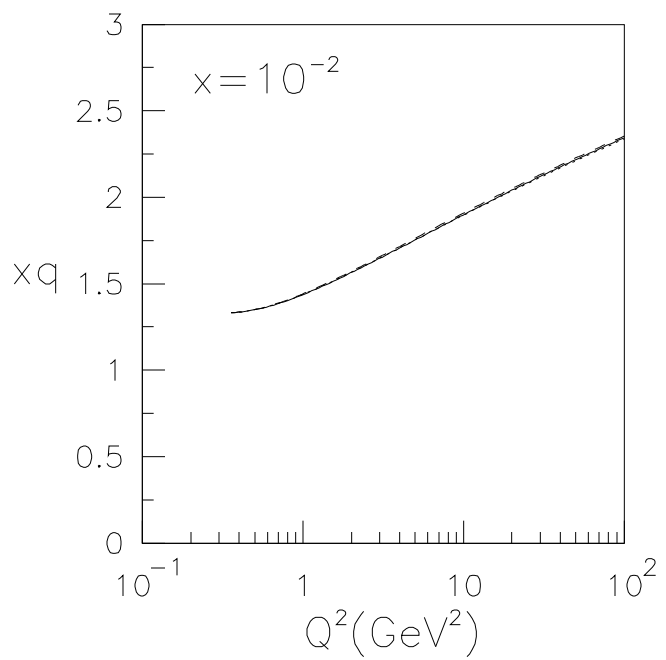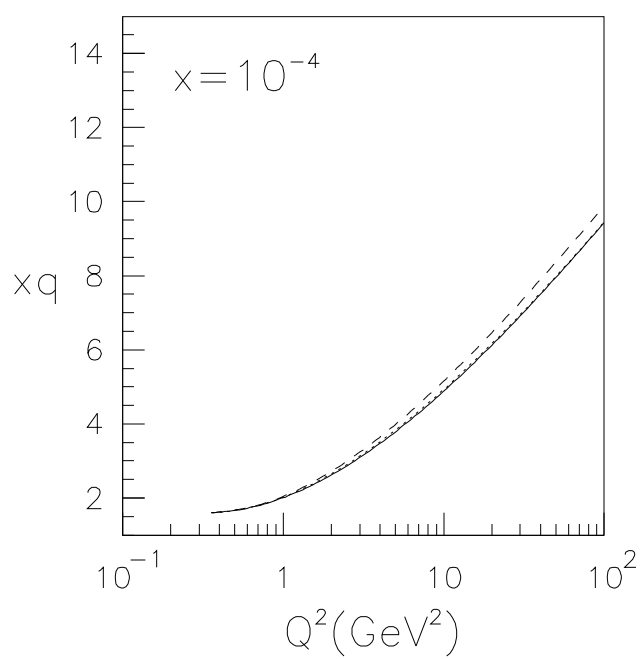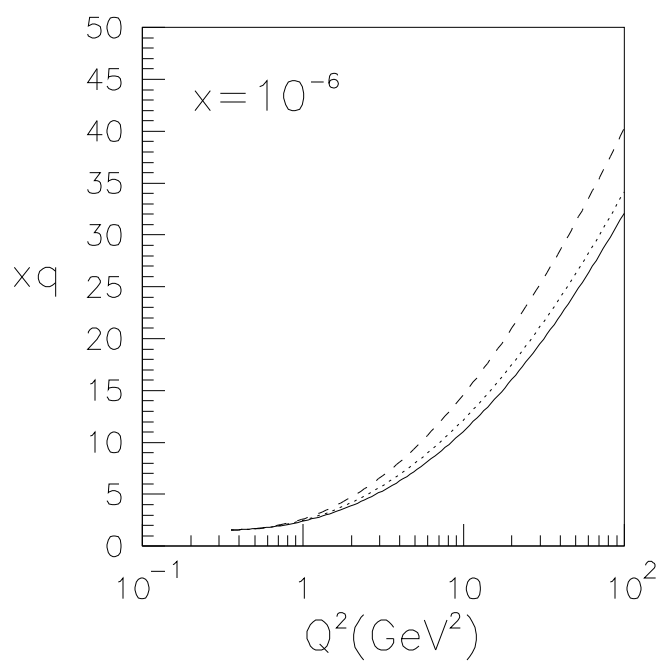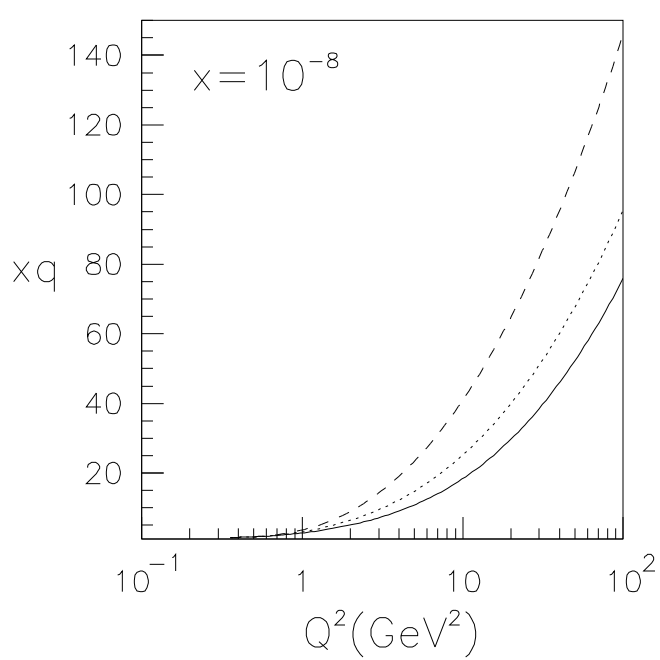
Fig.6
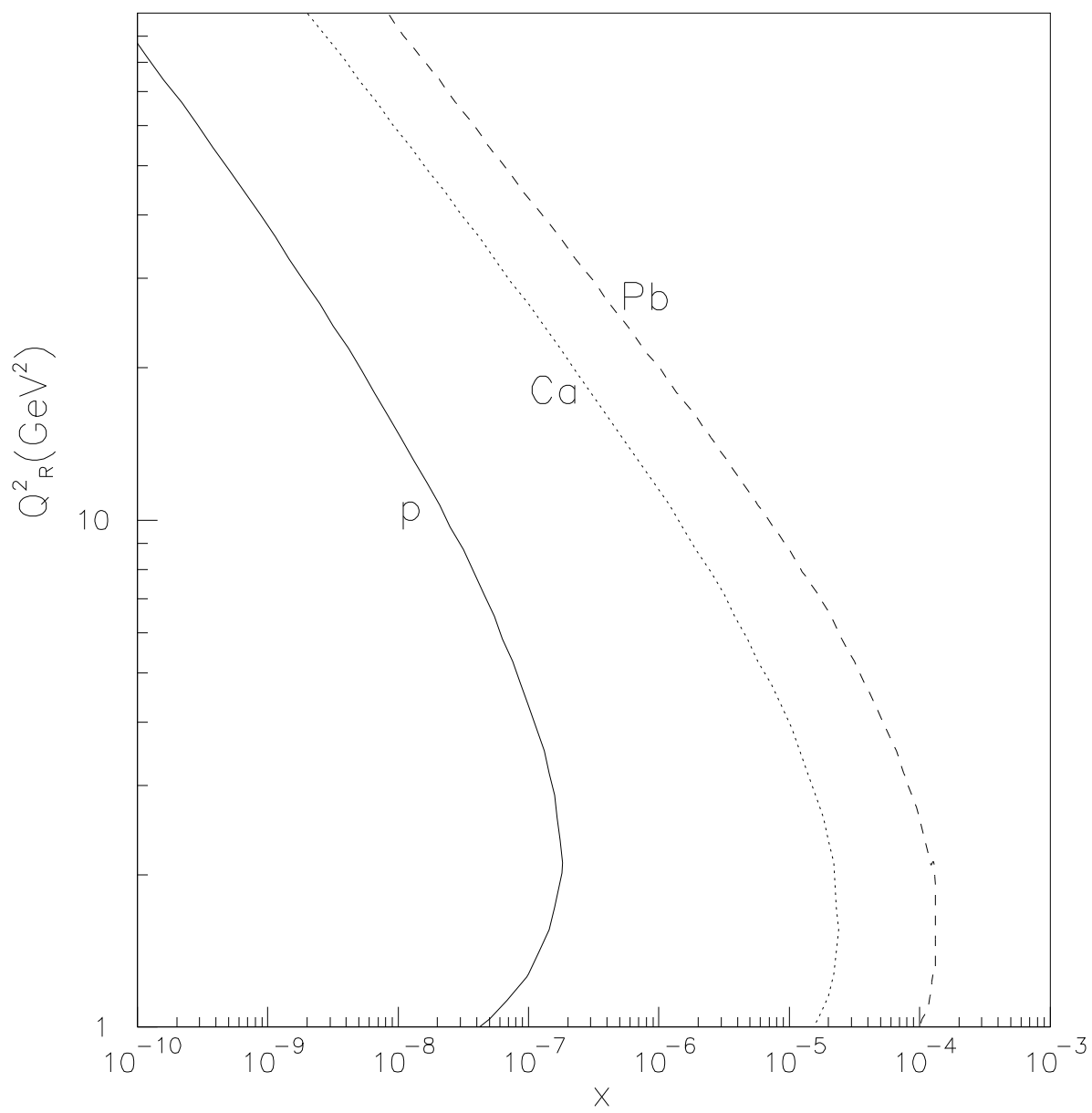
Fig.7
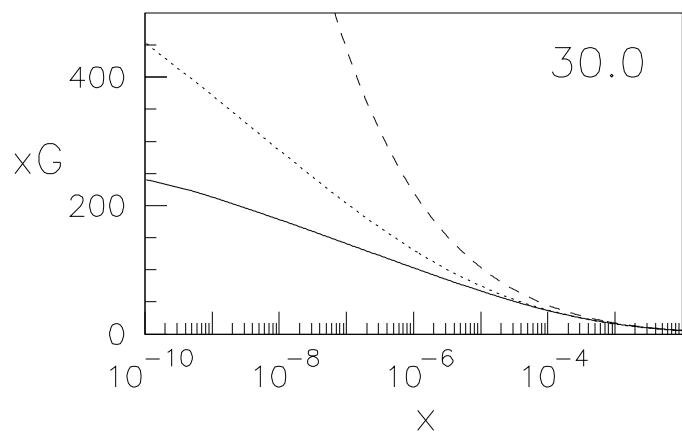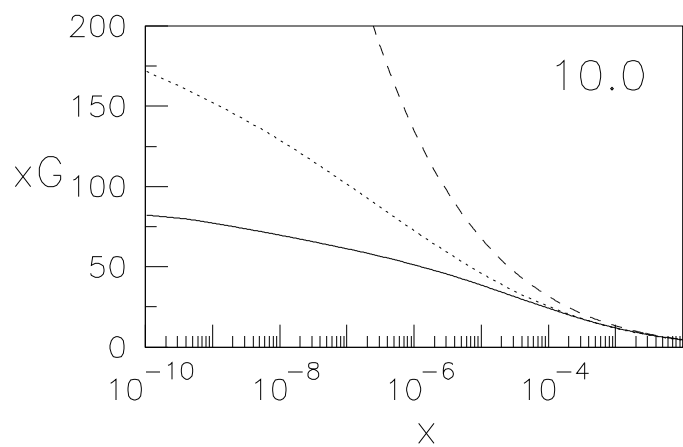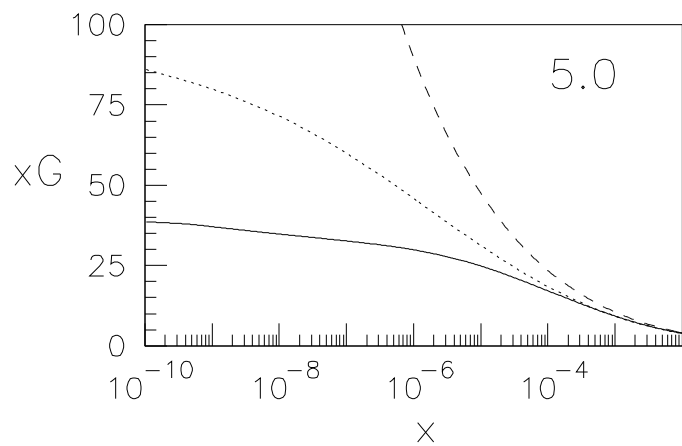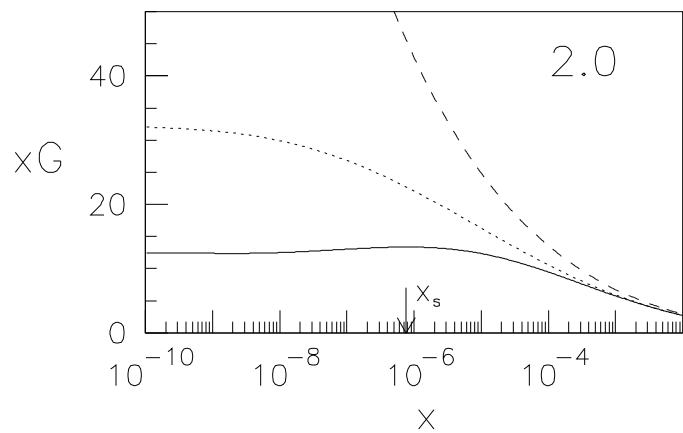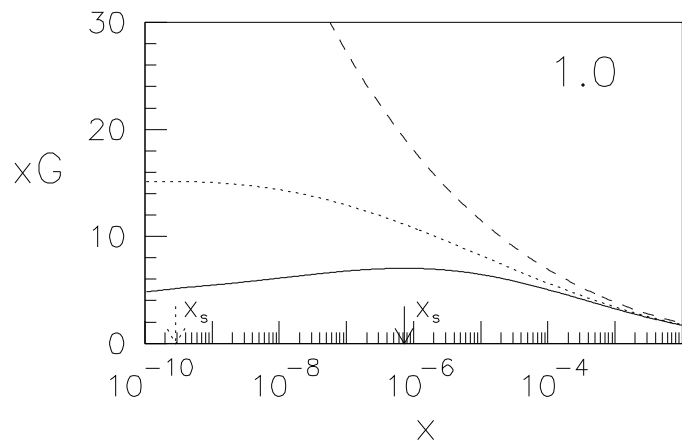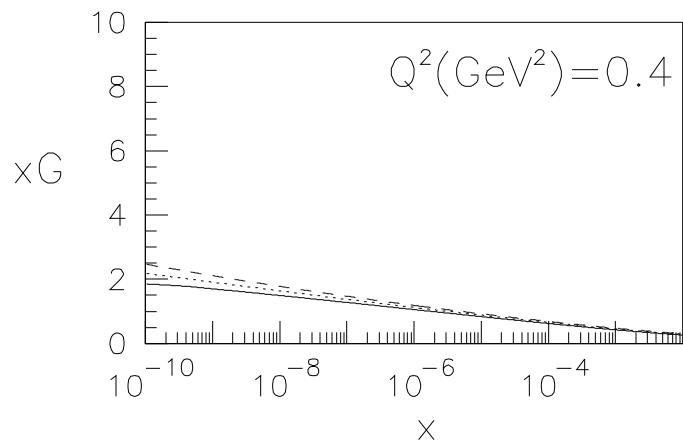
Fig.8
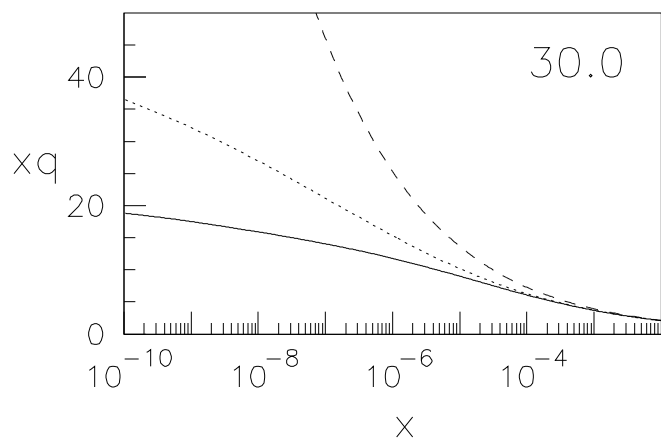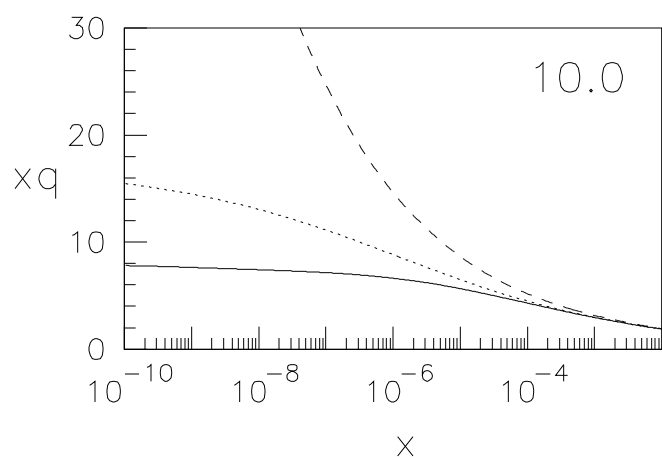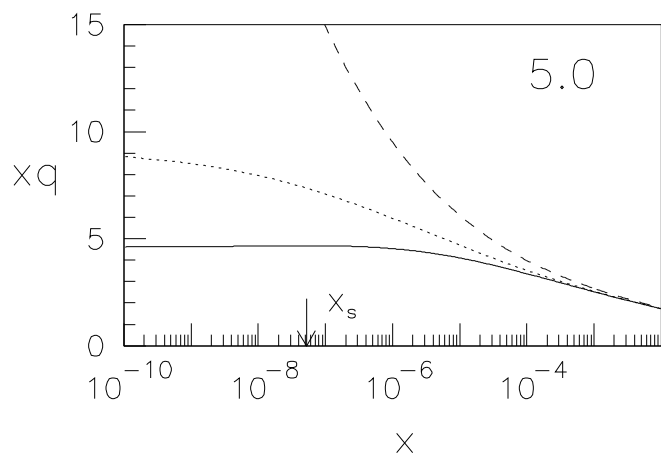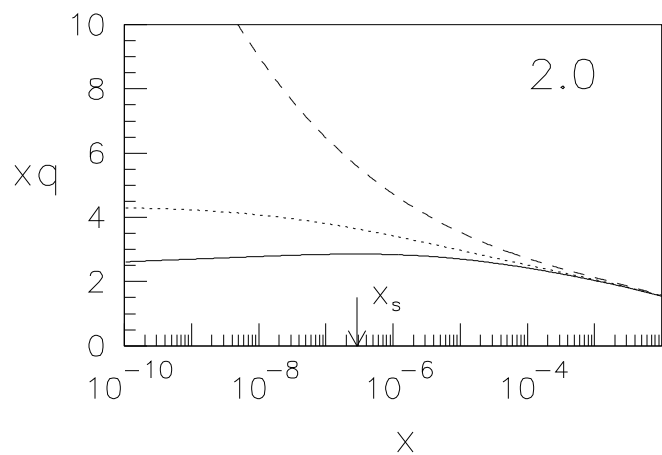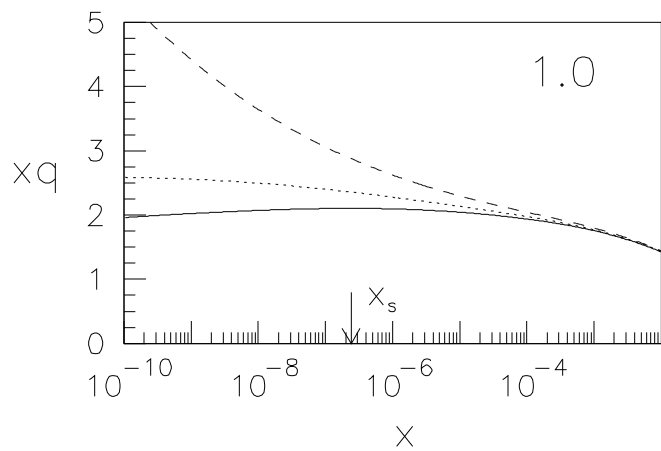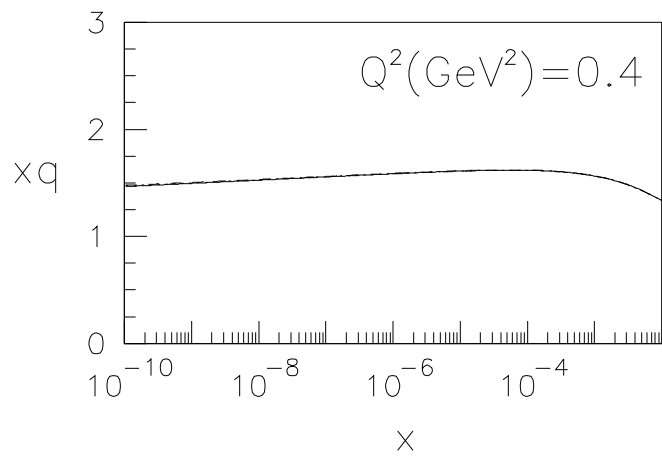
Fig.9
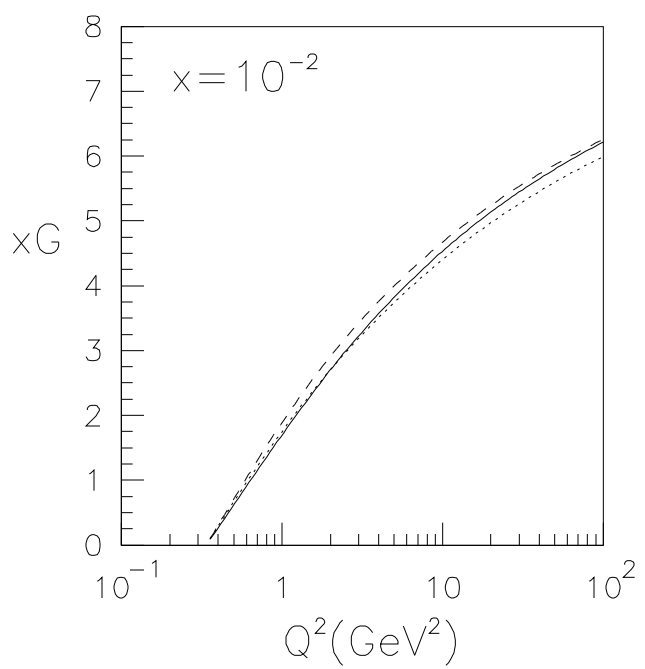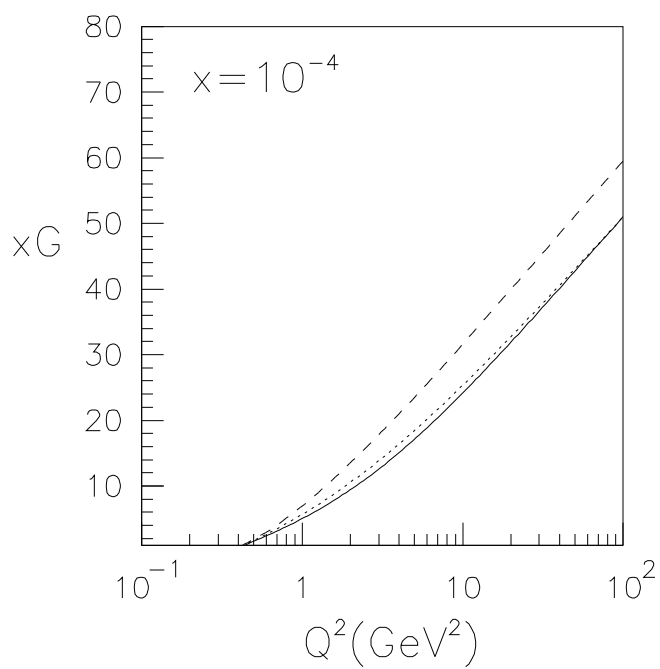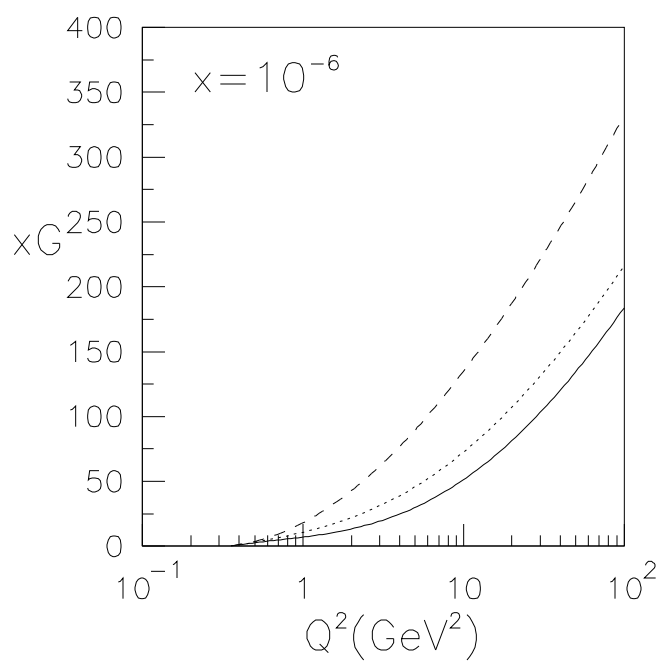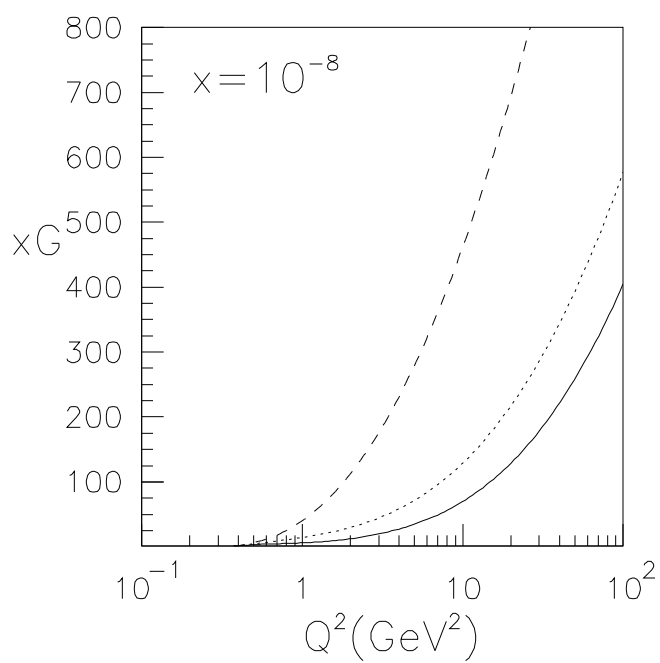
Fig.10
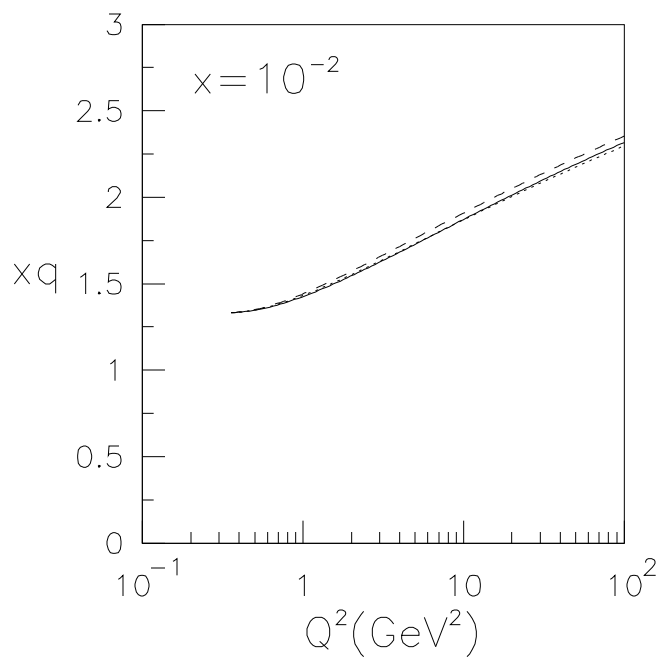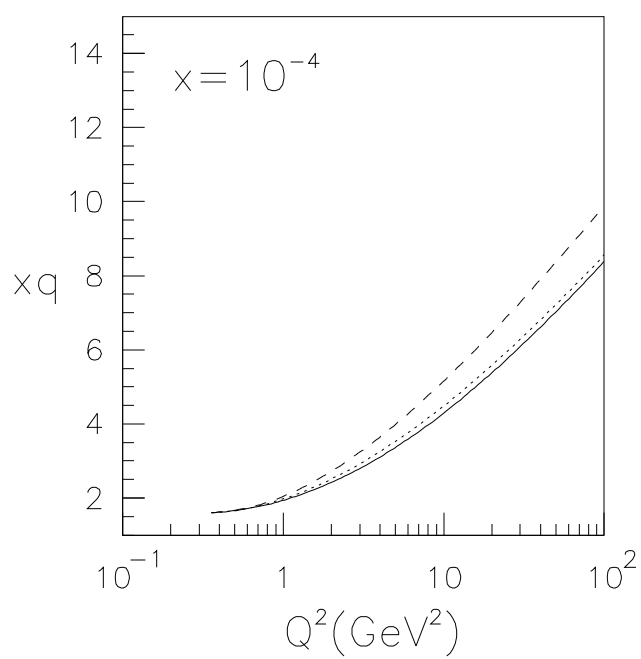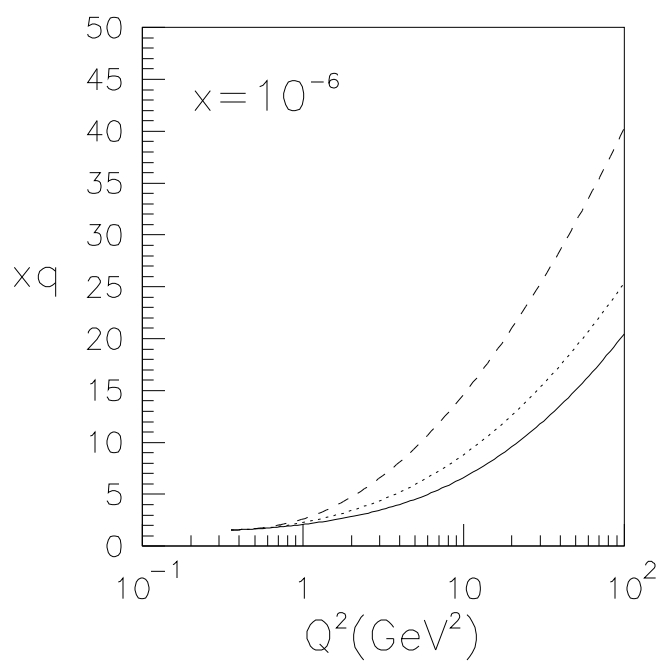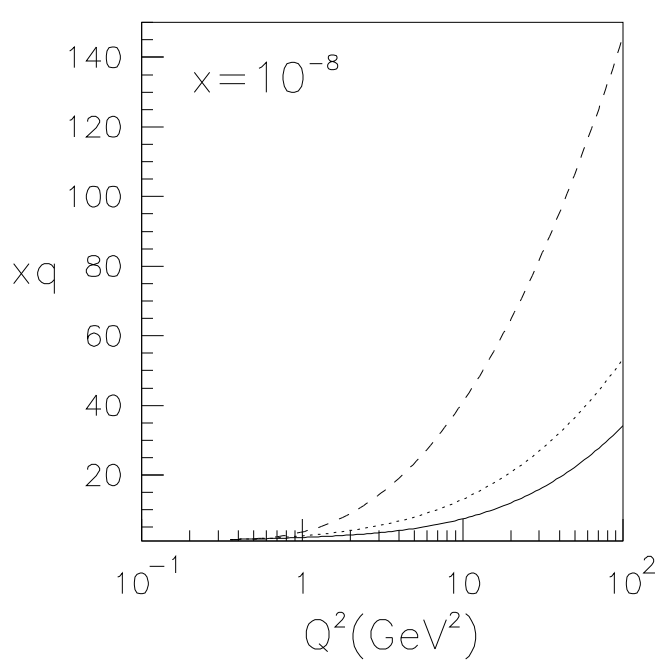
Fig.11
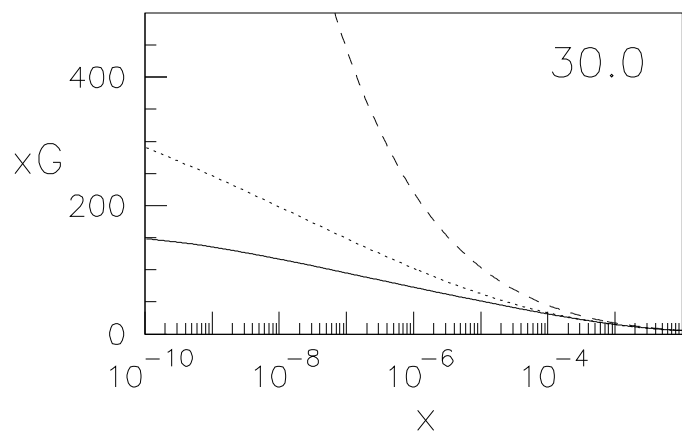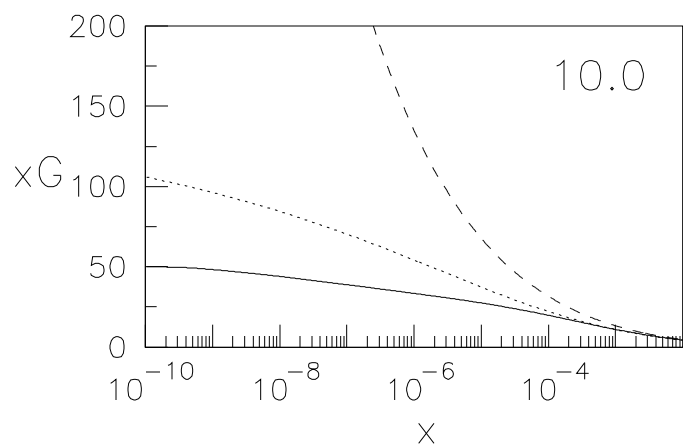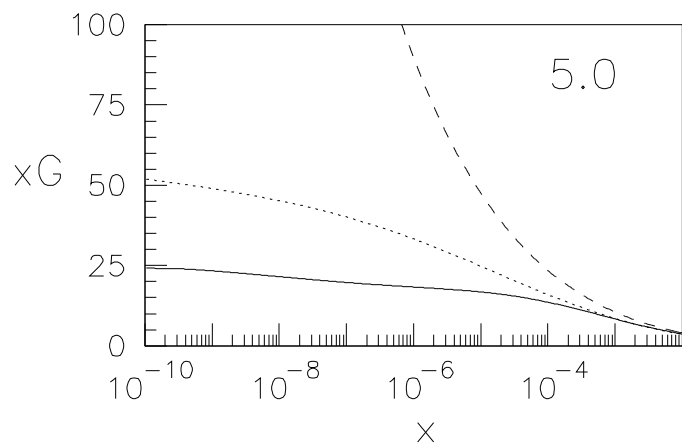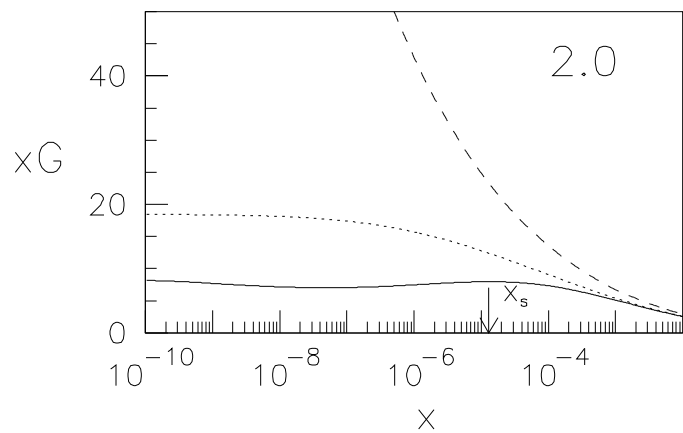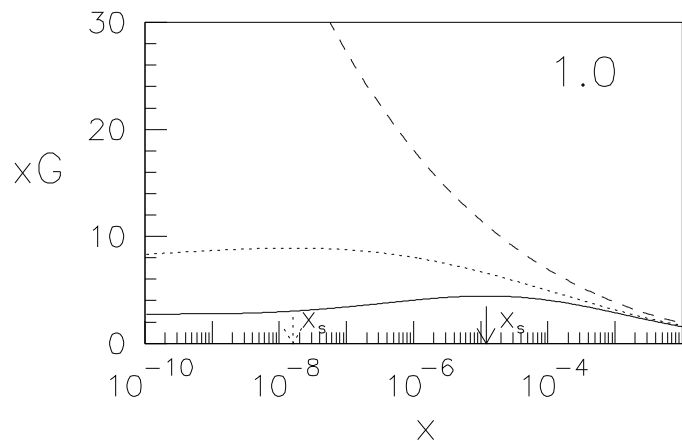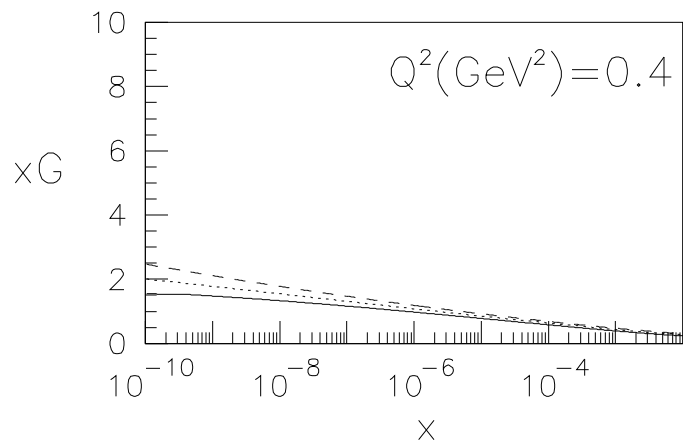
Fig.12
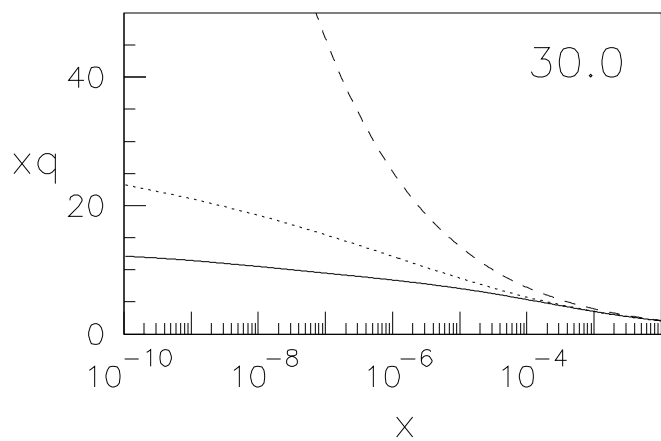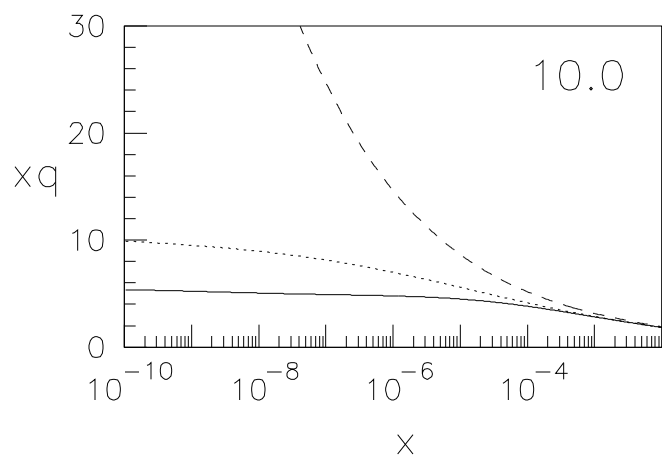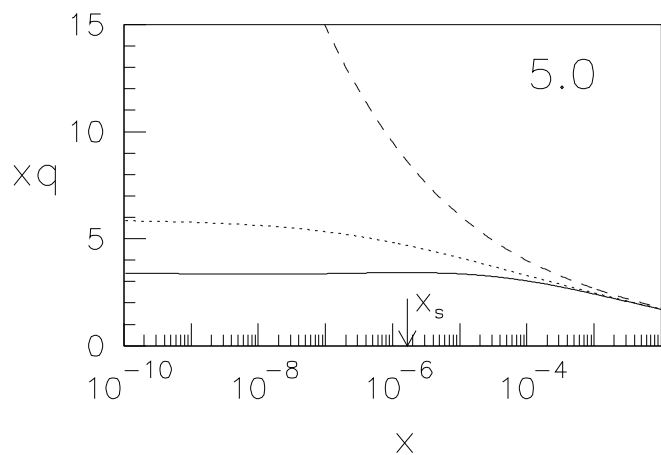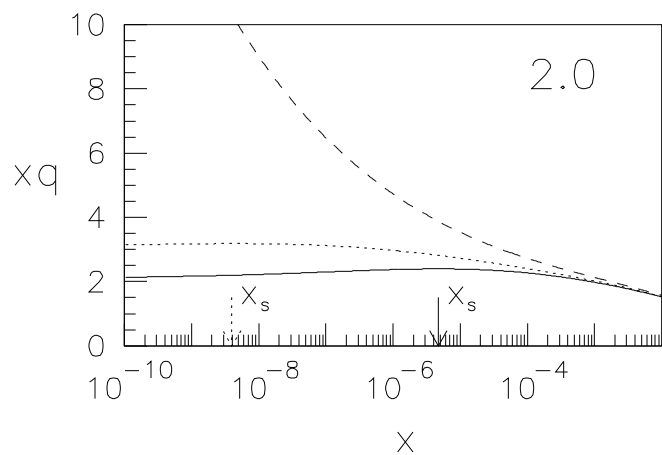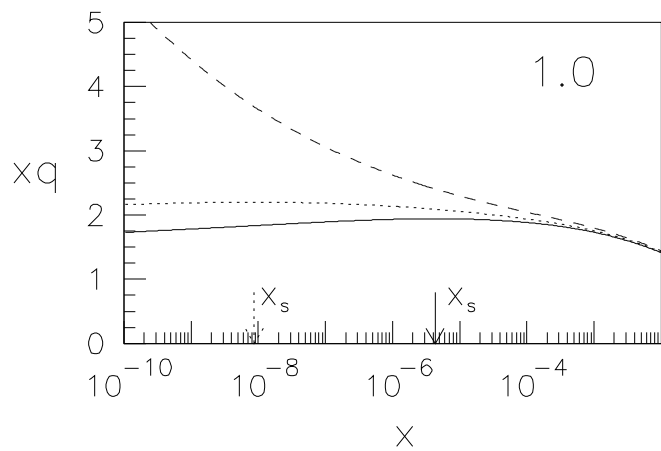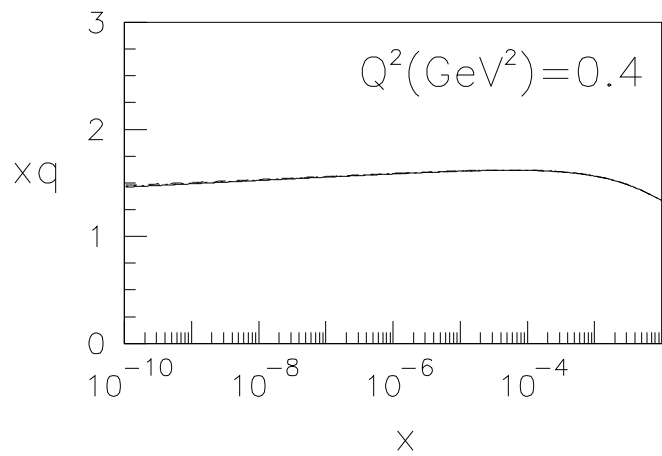
Fig.13
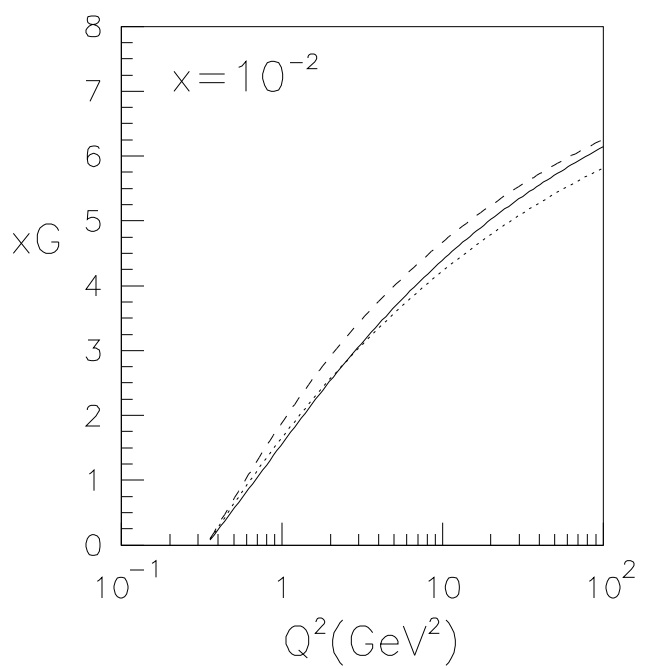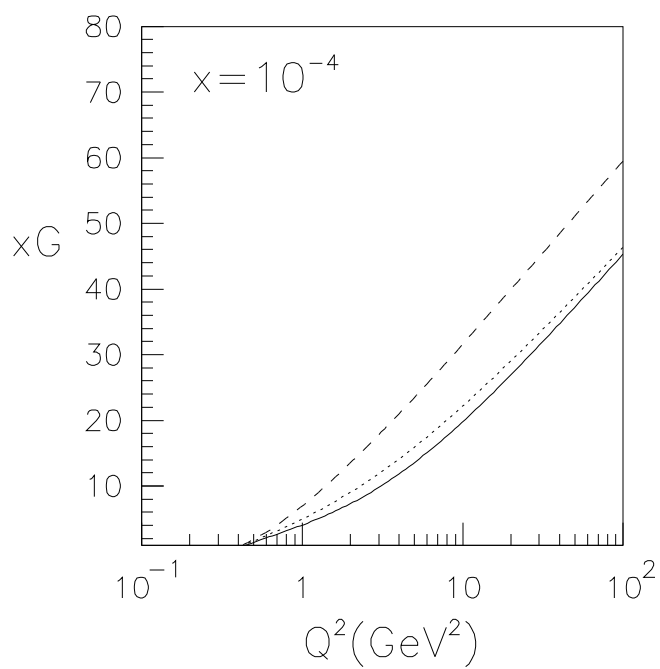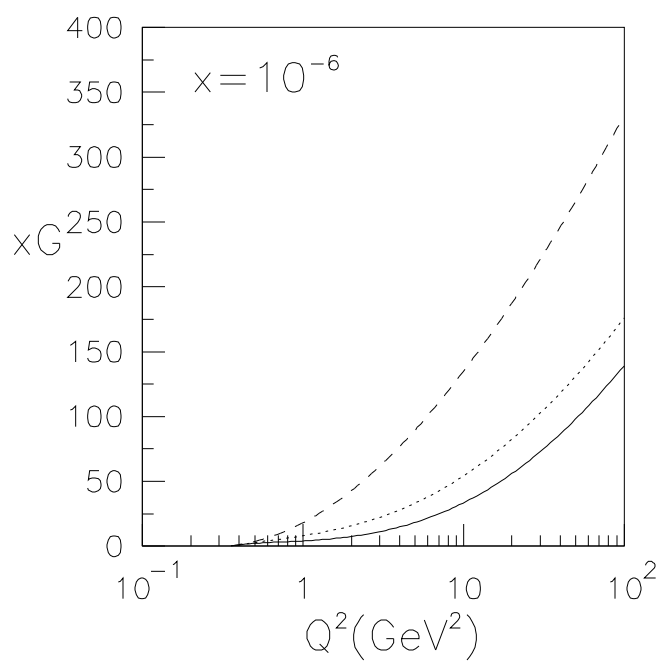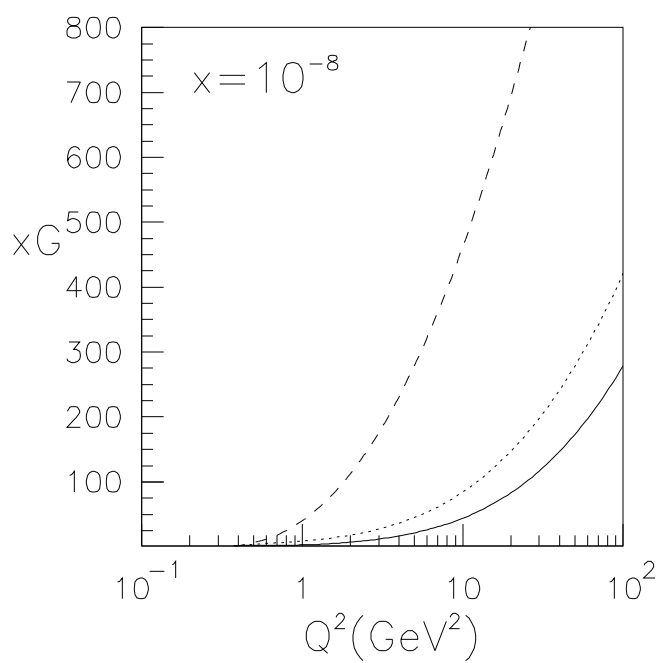
Fig.14
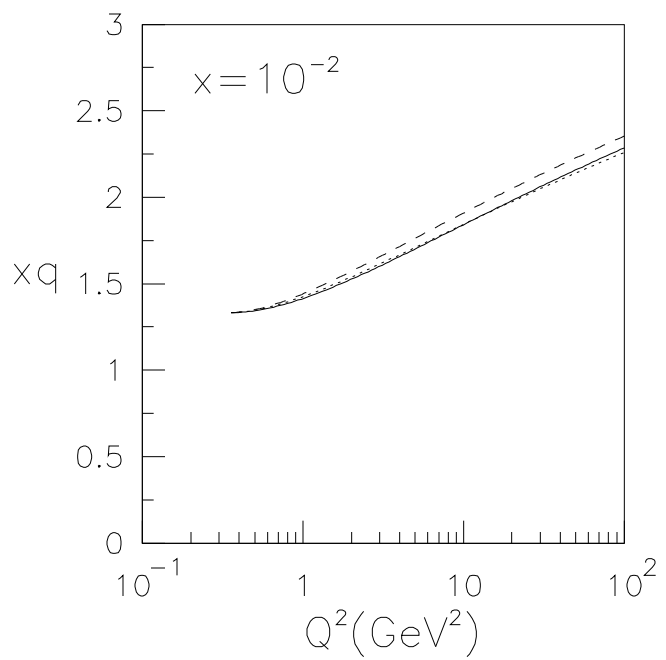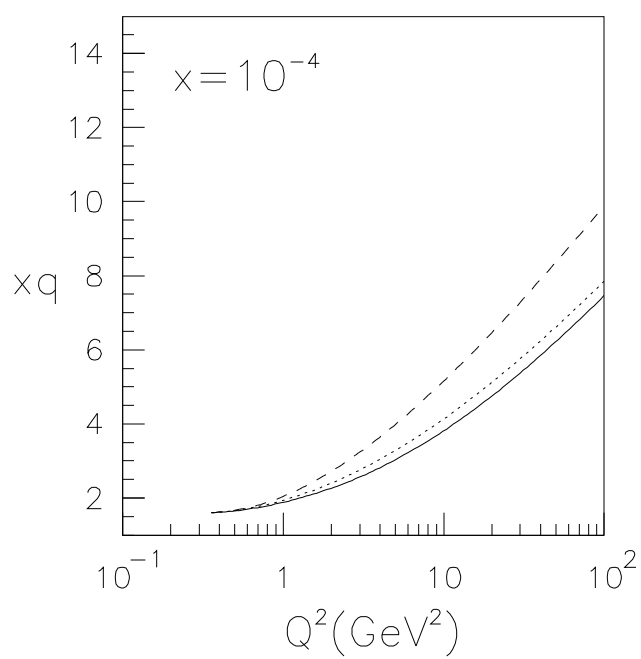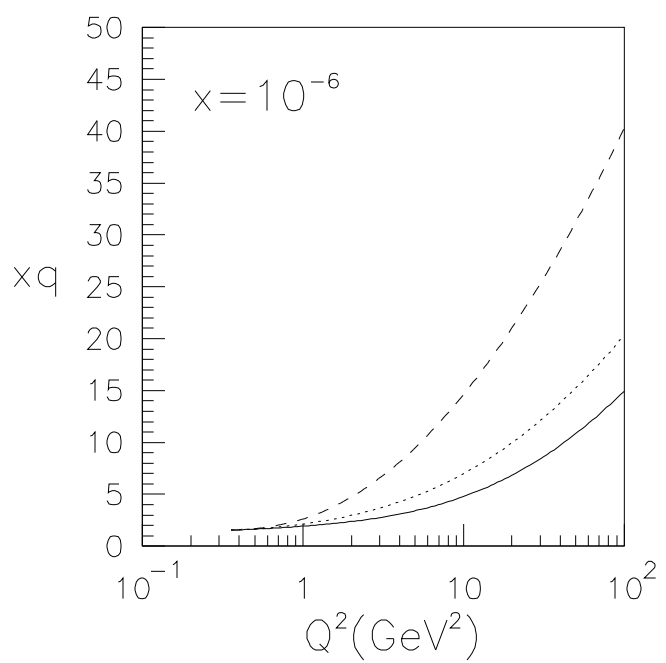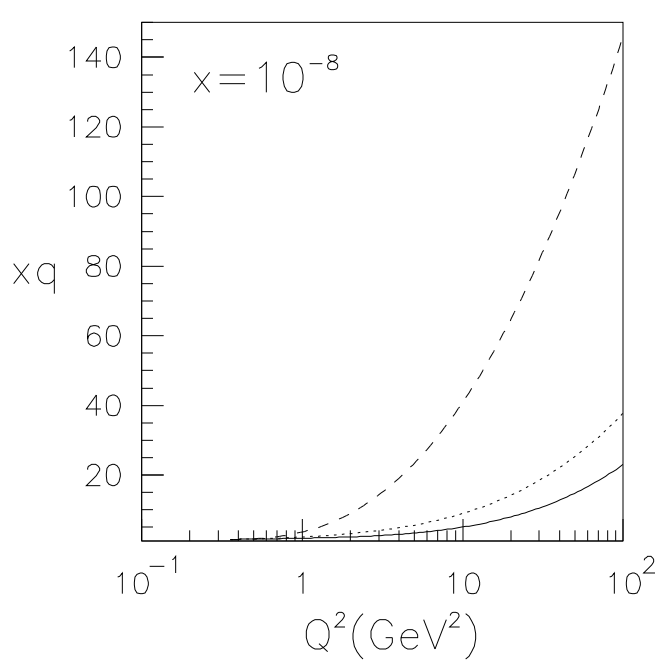
Fig.15
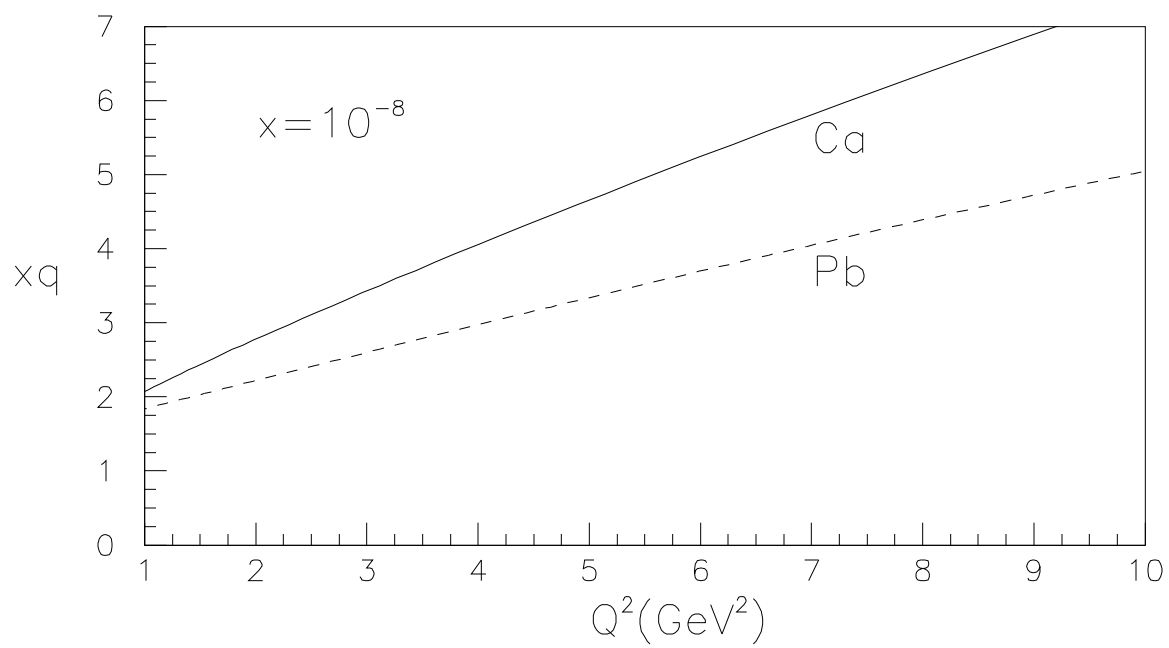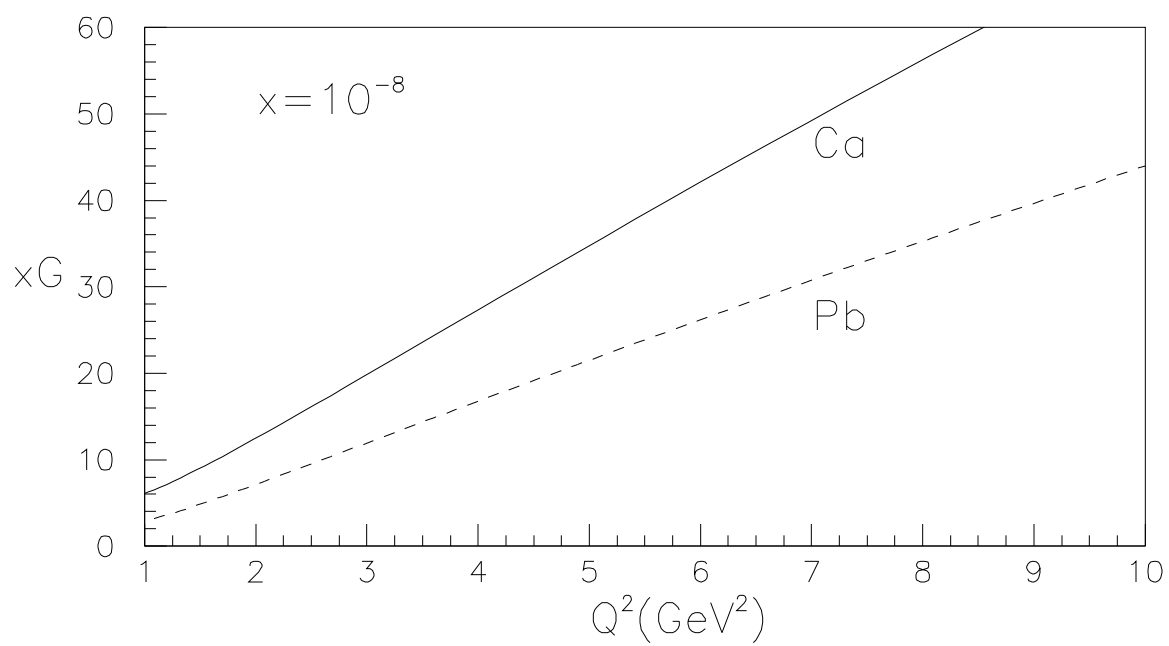
Fig.16
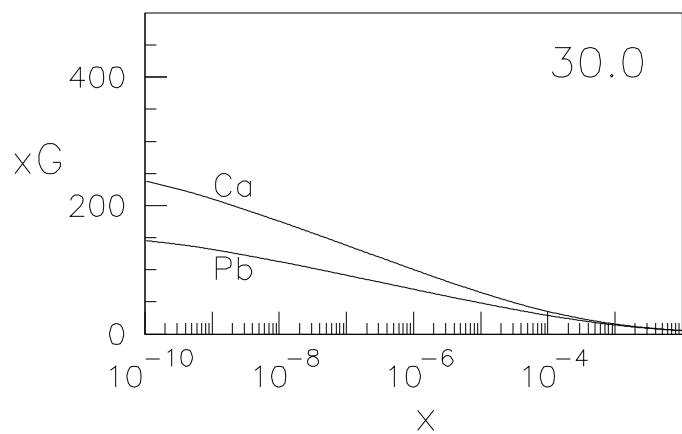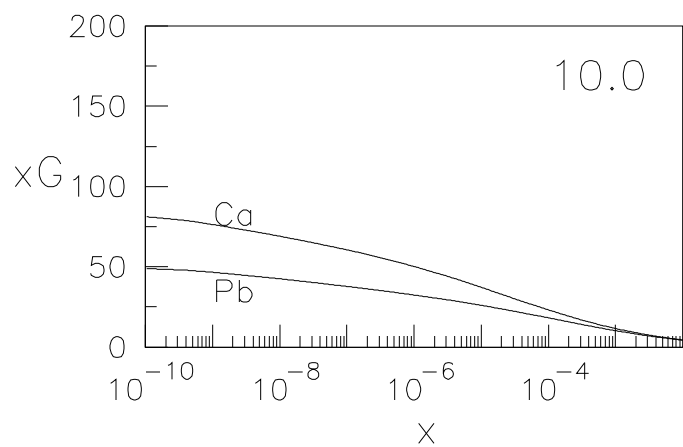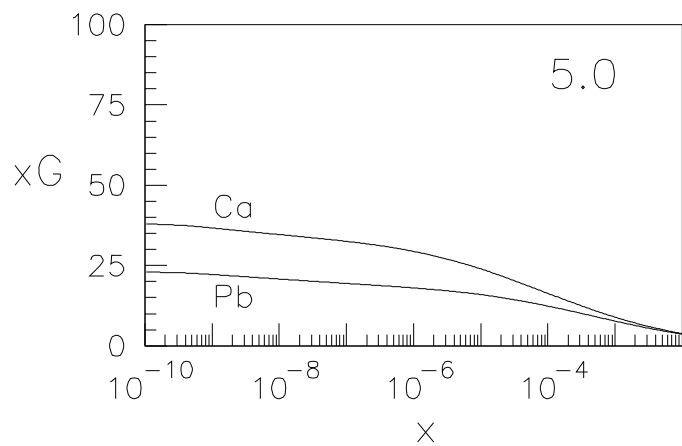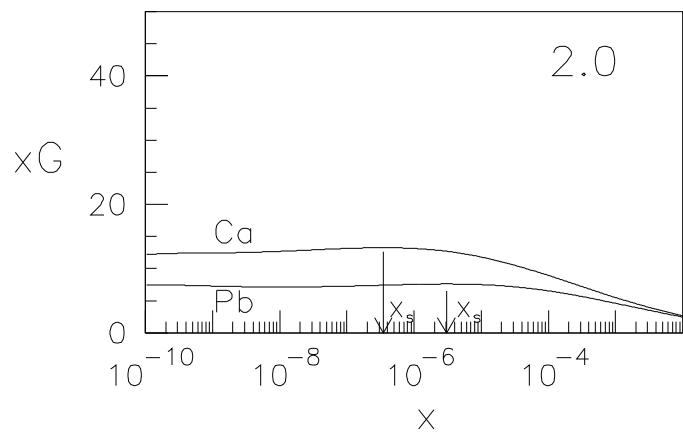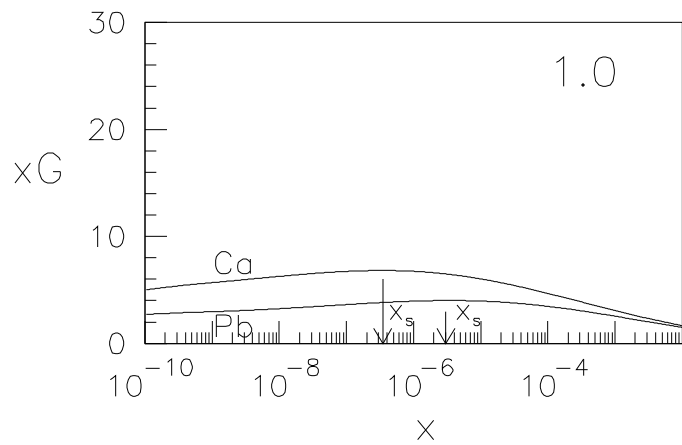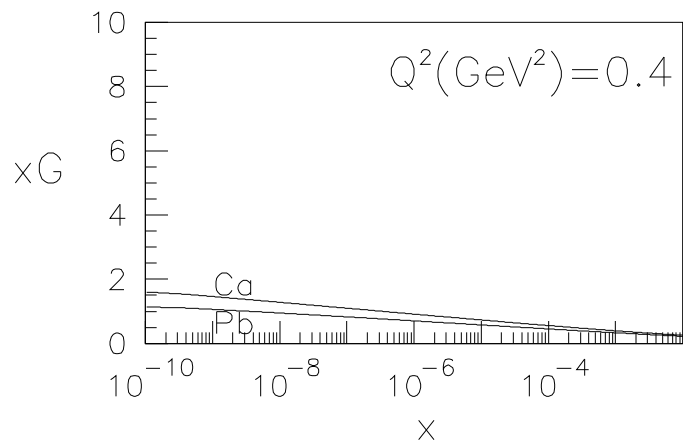
Fig.17

Fig.18

Fig.19

Fig.20

Fig.21